Influence of Stratosphere Polar Vortex Variability on the Mesosphere, Thermosphere, and Ionosphere

Nicholas Michael Pedatella[1]

[1]National Center for Atmospheric Research (UCAR)

March 26, 2023

Abstract

The Whole Atmosphere Community Climate Model with thermosphere-ionosphere eXtension (WACCM-X) is used to investigate the influence of stratosphere polar vortex variability on the mesosphere, thermosphere, and ionosphere during Northern Hemisphere winter. Based on 40 simulated Northern Hemisphere winters, the mesosphere and lower thermosphere (MLT) residual circulation is found to depend on whether the stratosphere polar vortex is strong or weak. In particular, during weak stratosphere polar vortex time periods, the MLT circulation anomalies are characterized by clockwise and anti-clockwise flow in the Northern and Southern Hemispheres, respectively. Opposite, though weaker, anomalies are found to occur during time periods when the stratosphere polar vortex is strong. The MLT circulation anomalies influence the composition of the lower thermosphere, leading to ±5% changes in the thermosphere column integrated atomic oxygen to molecular nitrogen ratio (O/N2). Large differences between strong and weak stratosphere polar vortex events are also found to occur in the semidiurnal migrating tide (SW2) in the MLT, which leads to ±15-20% differences in the SW2 component of the ionosphere total electron content (TEC) at low latitudes. The WACCM-X simulation results indicate that variability in the stratosphere polar vortex can explain ˜30% and ˜18% of the quiet time variability in thermosphere O/N2 and the SW2 component of TEC during Northern Hemisphere winter, respectively.

Influence of Stratosphere Polar Vortex Variability on the Mesosphere, Thermosphere, and Ionosphere

N. M. Pedatella[1,2]

[1]High Altitude Observatory, National Center for Atmospheric Research, Boulder, CO, USA.
[2]COSMIC Program Office, University Center for Atmospheric Research, Boulder, CO, USA.

Key Points:

- Investigate the impact of stratosphere polar vortex on the mesosphere and lower thermosphere circulation, ionosphere, and thermosphere.
- Residual circulation in the mesosphere and lower thermosphere is impacted by both strong and weak stratosphere polar vortex events.
- Stratosphere polar vortex explains ∼30% and ∼18% of quiet time variability in thermosphere O/N_2 and ionosphere SW2, respectively.

Corresponding author: Nicholas Pedatella, `nickp@ucar.edu`

Abstract

The Whole Atmosphere Community Climate Model with thermosphere-ionosphere eXtension (WACCM-X) is used to investigate the influence of stratosphere polar vortex variability on the mesosphere, thermosphere, and ionosphere during Northern Hemisphere winter. Based on 40 simulated Northern Hemisphere winters, the mesosphere and lower thermosphere (MLT) residual circulation is found to depend on whether the stratosphere polar vortex is strong or weak. In particular, during weak stratosphere polar vortex time periods, the MLT circulation anomalies are characterized by clockwise and anti-clockwise flow in the Northern and Southern Hemispheres, respectively. Opposite, though weaker, anomalies are found to occur during time periods when the stratosphere polar vortex is strong. The MLT circulation anomalies influence the composition of the lower thermosphere, leading to $\pm 5\%$ changes in the thermosphere column integrated atomic oxygen to molecular nitrogen ratio (O/N_2). Large differences between strong and weak stratosphere polar vortex events are also found to occur in the semidiurnal migrating tide (SW2) in the MLT, which leads to $\pm$15-20% differences in the SW2 component of the ionosphere total electron content (TEC) at low latitudes. The WACCM-X simulation results indicate that variability in the stratosphere polar vortex can explain $\sim$30% and $\sim$18% of the quiet time variability in thermosphere O/N_2 and the SW2 component of TEC during Northern Hemisphere winter, respectively.

1 Introduction

During Northern Hemisphere winter, the stratosphere polar vortex that forms at high-latitudes in the Northern Hemisphere exhibits considerable variability. The stratosphere polar vortex variability is largely due to the presence, or absence, of planetary wave activity. During periods of strong planetary wave activity, the stratosphere polar vortex is weakened, leading to the occurrence of sudden stratosphere warming (SSW) events (Matsuno, 1971). Though identified based on changes in the stratosphere, SSWs have a wide range of impacts throughout the atmosphere (Pedatella et al., 2018; Baldwin et al., 2020).

In the mesosphere and lower thermosphere (MLT), SSW events are associated with changes in the circulation, mean winds, and atmospheric tides. At middle to high latitudes in the Northern Hemisphere, the zonal winds in the MLT reverse direction during SSWs (Liu & Roble, 2002; Hoffmann et al., 2007), which is primarily attributed to changes in gravity wave forcing (Liu & Roble, 2002; Limpasuvan et al., 2016; Zülicke et al., 2018). These zonal wind changes can extend across the equator into the Southern Hemisphere MLT through inter-hemispheric coupling (Körnich & Becker, 2010; Smith et al., 2020). The zonal mean zonal wind changes that occur during SSWs leads to enhancements in the migrating solar (SW2) and lunar (M2) semidiurnal tides (Pedatella et al., 2012; Zhang & Forbes, 2014; Chau et al., 2015). The SW2 is also enhanced due to changes in ozone forcing during SSWs (Siddiqui et al., 2019). Additional tidal variability occurs in non-migrating semidiurnal tides due to the non-linear interactions between the migrating tides and enhanced planetary wave activity (Liu et al., 2010; Pedatella & Liu, 2013; He et al., 2017). The changes in wave forcing during SSWs, including from gravity waves, planetary waves, and tides, alter the mean circulation of the MLT. During SSWs, the MLT circulation is characterized by enhanced clockwise and anti-clockwise circulation patterns in the Northern and Southern Hemispheres, respectively (Miyoshi et al., 2015; Limpasuvan et al., 2016; Orsolini et al., 2022).

The changes that occur in the MLT circulation and tides during SSWs have subsequent effects on the ionosphere and thermosphere. In the equatorial and low latitude ionosphere, there is a pronounced change in the electric fields, vertical plasma drift velocities, and electron densities (Chau et al., 2009; Fejer et al., 2010; Goncharenko et al., 2010). These effects are predominantly driven by changes in the solar and lunar semidiurnal tides and their impact on the E-region dynamo (Fang et al., 2012; Maute et al., 2014). Variations in F-region electron densities also occur at middle latitudes, and are thought to be due to the propagation of enhanced semidiurnal tides into the F-region (Fagundes et al., 2015; Pedatella & Maute, 2015). The magnitude of the ionosphere variations during SSWs can be large, reaching, or even exceeding, 50-100% of climatological values. In contrast, smaller variations (~5-10%) are observed in the thermosphere neutral composition (atomic Oxygen to molecular Nitrogen ratio, O/N_2) and neutral density (Yamazaki et al., 2015; Oberheide et al., 2020). The thermosphere composition and density changes during SSWs arise due to the aforementioned changes in MLT circulation (Pedatella et al., 2016; Jr. et al., 2020). For a detailed discussion on the effects of SSWs on the middle and upper atmospheres, the reader is referred to the review papers by Chau et al. (2012), Yiğit et al. (2016), and Goncharenko et al. (2021),

The understanding of stratosphere polar vortex variability on the mesosphere, thermosphere, and ionosphere has largely focused on SSW events. However, recent studies have demonstrated that there is a continuum of variability in the middle and upper atmosphere associated with variations in the stratosphere polar vortex. Based on Specified Dynamics Whole Atmosphere Community Climate Model with thermosphere-ionosphere eXtension (SD-WACCM-X) simulations, Pedatella and Harvey (2022) demonstrated that, in addition to weak stratosphere polar vortex events (i.e., SSWs), time periods characterized by a strong stratosphere polar vortex also lead to anomalous zonal mean temperature, winds, and tides in the MLT. Of interest to the present investigation is that Pedatella and Harvey (2022) found the SW2 at middle latitudes in the MLT to be well correlated with the strength of the stratosphere polar vortex across the full range of stratosphere polar vortex variability. This is consistent with Liu (2014), who found a strong correlation between SW2 and zonal mean zonal winds in the high latitude stratosphere. Oberheide (2022) also found a close relationship between the stratosphere polar vortex variability and the SW2 in ionosphere electron density, demonstrating that the influence of the stratosphere polar vortex variability on the SW2 in the MLT subsequently impacts the ionosphere. The strength of the stratosphere polar vortex has also been found to modulate gravity wave activity in the thermosphere and the associated traveling ionosphere disturbances (Frissell et al., 2016; Becker et al., 2022). Specifically, a strong stratosphere polar vortex was found to lead to an enhancement in TIDs while a weak stratosphere polar vortex decreased TID activity.

The present study aims to further investigate how the range of stratosphere polar vortex variability influences the mesosphere, thermosphere, and ionosphere, including both strong and weak stratosphere polar vortex time periods. This is investigated using 40 Northern Hemisphere winters simulated by WACCM-X. The WACCM-X simulations are used to elucidate the influence of strong and weak stratosphere polar vortex time periods on the MLT circulation, thermosphere composition, and ionosphere electron density. The results demonstrate that variability in the stratosphere polar vortex is an important driver of the day-to-day variability in the middle and upper atmosphere during Northern Hemisphere winter, and that these effects are not limited to SSW time periods.

2 WACCM-X Simulations

Analysis of the impact of stratosphere polar vortex variability in the mesosphere, thermosphere, and ionosphere is investigated based on free-running WACCM-X simulations. WACCM-X is a whole atmosphere model that simulates the chemistry, dynamics, electrodynamics, and physics of the Earth's atmosphere from the surface to the upper thermosphere (4.1×10^{-10} hPa). The model horizontal resolution is 1.9° in latitude and 2.5° in longitude. The vertical resolution is ~1-3 km up to 0.96 hPa, and 0.25 scale heights above this level. A detailed description of WACCM-X can be found in Liu et al. (2018) and is not repeated herein.

The simulations for the present study consist of an ensemble of 40 Northern Hemisphere winters simulated by WACCM-X in its free-running mode. The simulations were initialized from an identical state on October 1. Random perturbations were applied to the model temperature fields at the start of the simulations, which leads to the ensemble members simulating different weather conditions due to chaotic divergence (Liu et al., 2009; Pedatella & Liu, 2018). To eliminate any influence of solar and geomagnetic activity, the simulations were performed with a constant solar flux of 70 solar flux units and a K_p of 0^+. Similar to Pedatella and Harvey (2022), we use the Northern Annular Mode (NAM) at 10 hPa as a measure of the strength of the stratosphere polar vortex. The NAM is calculated based on the polar cap (>65°N) average geopotential height anomalies (Gerber & Martineau, 2018). It is important to note that the NAM in the present study may not be reflective of the true NAM due to the NAM being normalized by the annual mean and the present simulations only covering a portion of the year. As shown in Figure 1, this may lead to a slight difference in the stratosphere (10 hPa) NAM distribution in the WACCM-X ensemble simulations compared to MERRA-2. The different NAM distributions may also be related to differences in the stratosphere zonal mean zonal winds at 10 hPa and 60°N (Figure 1a). In particular, the WACCM-X wind distribution is narrower, which may be related to either fewer mid-winter SSWs simulated in WACCM and/or natural variability (de la Torre et al., 2012; Garcia et al., 2017). This will lead to a narrower NAM distribution as seen in Figure 1b. Given the narrower NAM distribution, the thresholds for strong and weak stratosphere polar vortex events are chosen to be +1.5 and -2.0, respectively. This leads to a roughly similar fraction of strong (13.3%) and weak (4.4%) events as in MERRA-2 when using the thresholds of +2.0 and -3.0 (Pedatella & Harvey, 2022). Similar to Pedatella and Harvey (2022), we present anomalies from the climatology, where the climatology is based on the 40 Northern Hemisphere winter average smoothed with a running 20-day mean. A Student's T-test is used to test the anomalies for statistical significant relative to the anomalies when the stratosphere polar vortex is consider to be neither weak nor strong.

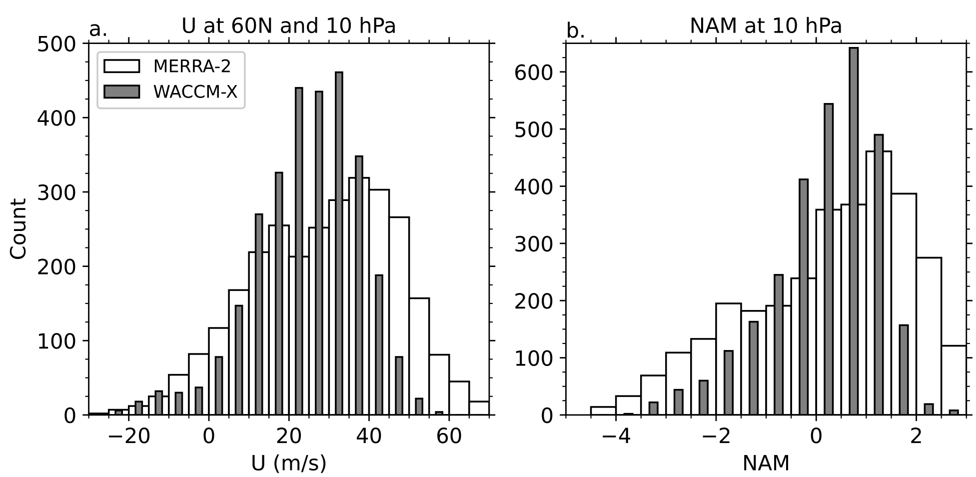

Figure 1. Distribution of (a) zonal mean zonal winds at 60°N and 10 hPa and (b) Northern Annular Mode (NAM) index at 10 hPa during December 15 to March 1 in MERRA-2 (white) and WACCM-X (grey).

3 Results and Discussion

3.1 Mesosphere and Lower Thermosphere

Figure 2 shows the average zonal mean temperature and zonal wind anomalies during strong and weak stratosphere polar vortex time periods. The anomalies are consistent in both magnitude and spatial structure with the results of Pedatella and Harvey (2022). However, the results of Figure 2 are extended into the thermosphere, revealing the temperature and wind anomalies at thermosphere altitudes. They show the expected stratosphere warming, mesosphere cooling, and lower thermosphere warming at high latitudes in the Northern Hemisphere during weak stratosphere polar vortex time periods (e.g., Liu & Roble, 2002), with weaker and opposite signed anomalies during strong stratosphere polar vortex time periods. Extension of the temperature anomalies across the equator into the Southern Hemisphere MLT is also evident. Though there are some minor differences in the equatorial upper stratosphere and lower mesosphere, the zonal mean zonal wind anomalies are also consistent with Pedatella and Harvey (2022). The 40 Northern Hemisphere winters simulated by the free-running WACCM-X thus reproduce the zonal mean anomalies found previously in SD-WACCM-X, which were also shown to be consistent with Aura Microwave Limb Sounder observations. The zonal mean temperature and wind anomalies in Figure 2 reveal anomalies in the middle to upper thermosphere, which were not shown previously in Pedatella and Harvey (2022). During weak stratosphere polar vortex time periods, the thermosphere temperature decreases by $\sim$3-5 K at middle to high latitudes in both hemispheres, and increases by $\sim$2 K at low latitudes. In the thermosphere, the global average temperature decreases by $\sim$2 K, consistent with the observed decrease in satellite drag and neutral mass density (Yamazaki et al., 2015). The decrease is, however, smaller than observed by Yamazaki et al. (2015). A similar temperature pattern, with an increase at low latitudes and decrease at middle to high latitudes, was found to occur due to the influence of atmospheric tides by Jr. et al. (2016). Enhanced semidiurnal tidal amplitudes during weak stratosphere polar vortex time periods may thus explain the temperature structure seen in Figure 2a. In the middle to upper thermosphere, the zonal mean zonal wind anomalies during weak stratosphere polar vortex time periods are westward with maxima of $\sim$10 m/s at middle latitudes near 10^{-5} hPa. This is consistent with previous simulation results (e.g., Pedatella et al., 2016), and is thought to the related to the dissipation of SW2 in the middle thermosphere as will be discussed later. The temperature and zonal wind anomalies in the thermosphere during strong stratosphere polar vortex time periods are small ($<$ 2-3 K or m/s) and generally opposite to those that occur during weak stratosphere polar vortex time periods.

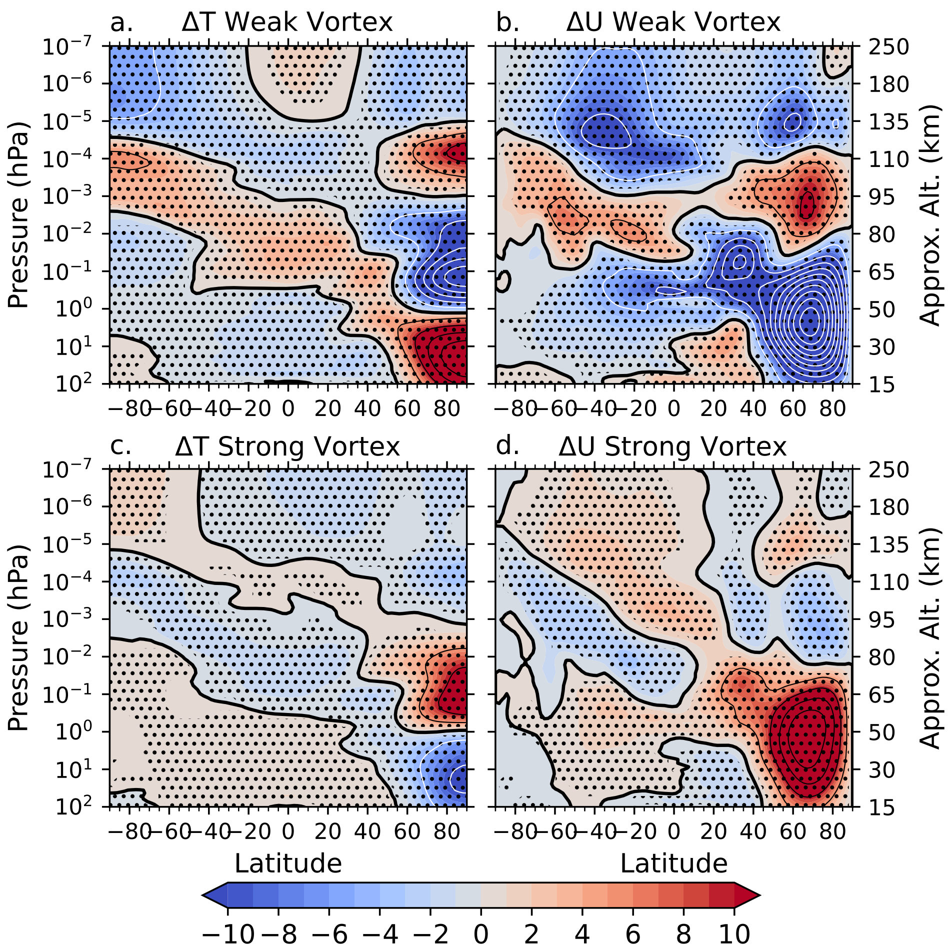

Figure 2. WACCM-X zonal mean anomalies in (a) temperature during weak stratosphere polar vortex times, (b) zonal mean zonal wind during weak stratosphere polar vortex times, (c) temperature during strong stratosphere polar vortex times, and (d) zonal mean zonal wind during strong stratosphere polar vortex times. Stippling denotes areas that are statistically significant at the 95% confidence level. Units are K and m/s for temperature and zonal wind, respectively. Contour lines are every 5 K or m/s, and the thick black line is the zero contour.

Anomalies in the SW2 during strong and weak stratosphere polar vortex time periods are shown in Figure 3. The SW2 anomalies in zonal wind are again largely consistent with Pedatella and Harvey (2022) in the MLT. During weak stratosphere polar vortex time periods, the SW2 in both zonal and meridional wind shows large enhancements in middle latitudes in both hemispheres with maxima between 10^{-4}-10^{-5} hPa (110-130 km). The dissipation of SW2 will tend to drive a westward zonal wind, and the dissipation of the SW2 at these altitudes is thus considered to be a major contributor to the westward zonal mean zonal wind anomalies in Figure 2b. The SW2 enhancements tend to extend into the upper thermosphere. There is, however, a region of decreased SW2 in the Northern Hemisphere middle thermosphere. The decreased SW2 in the middle thermosphere is thought to be due to the impact of the changes in zonal mean zonal winds on the propagation of different Hough modes of SW2 (e.g., Jin et al., 2012). Since the vertical wavelength of the tide impacts its vertical propagation, a change in the dominant modes can change how effectively the SW2 propagates into the middle thermosphere. Changes in the modes of SW2 may also lead to destructive interference, reducing the tidal amplitude (Pedatella et al., 2021). The SW2 anomalies in meridional wind during weak stratosphere polar vortex time periods (Figure 3b) similarity show large enhancements at middle latitudes in the MLT. The additional equatorial enhancement in the SW2 in meridional wind is anticipated due to the latitudinal structure of the SW2 Hough modes being different in zonal and meridional wind (Forbes, 1982). The SW2 meridional wind anomalies exhibit decreased amplitudes at low to middle latitudes ($\sim \pm$10-40°) in the thermosphere, which again may be related to changes in the dominant SW2 Hough modes. The SW2 anomalies during strong stratosphere polar vortex time periods (Figures 3c and 3d) are opposite those of the weak stratosphere polar vortex time periods; however, the magnitudes are smaller. The mechanisms driving the tidal anomalies during weak stratosphere polar vortex time periods are thus acting in the reverse manner during strong stratosphere polar vortex time periods.

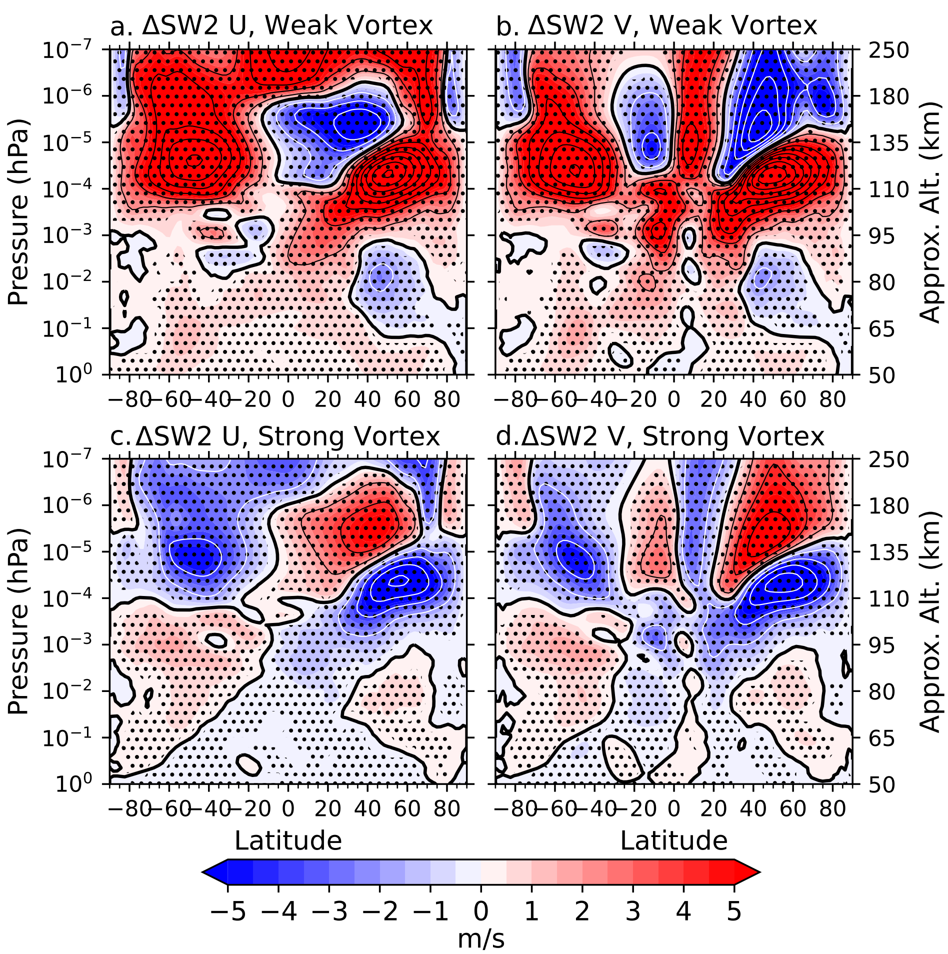

Figure 3. WACCM-X SW2 tidal amplitude anomalies during weak stratosphere polar vortex events for (a) zonal and (b) meridional wind. (c-d) Same as (a-b) except for during strong stratosphere polar vortex events. Stippling denotes areas that are statistically significant at the 95% confidence level. Contour lines are every 2 m/s, and the thick black line is the zero contour.

Changes in the residual meridional (v^*) and vertical ($w*$) circulation during strong and weak stratosphere polar vortex time periods are shown in Figure 4. During weak stratosphere polar vortex time periods, the residual meridional circulation in the Northern Hemisphere has southward anomalies between 10^{-1}-10^{-2} hPa (65-80 km) and northward anomalies at higher altitudes (10^{-3}-10^{-5} hPa, 95-120 km). The spatial structure and the magnitude of the anomalies are consistent with the anomalies that occur during SSWs (Orsolini et al., 2022). The anomalies stretch into the Southern Hemisphere with decreasing amplitude and the boundary between southward and northward anomalies increasing in altitude from the Northern to Southern Hemispheres. This leads to the meridional residual circulation anomalies being oppositely signed in the Northern and Southern Hemispheres at a fixed pressure level (or altitude). Considering also the vertical residual circulation anomalies, one can see that the circulation anomalies during weak stratosphere polar vortex time periods are characterized by a clockwise circulation in the MLT in the Northern Hemisphere, and an anti-clockwise circulation in the Southern Hemisphere MLT. This is again consistent with prior studies (Pedatella et al., 2016). A weak downwelling is also observed in the equatorial region, which is likely due to the dissipation of SW2 (Yamazaki & Richmond, 2013). The residual circulation anomalies during strong stratosphere polar vortex time periods (Figures 4c and 4d) are opposite signed compared to the weak stratosphere polar vortex time periods. The MLT circulation anomalies are thus anti-clockwise in the Northern Hemisphere and clockwise in the Southern Hemisphere during strong stratosphere polar vortex time periods. The reversed circulation anomalies indicates that the impacts of the circulation anomalies on, for example, thermosphere composition and mesosphere chemistry, during strong stratosphere polar vortex time periods will be opposite to those that occur during weak stratosphere polar vortex time periods, though the magnitude of the effects will be smaller.

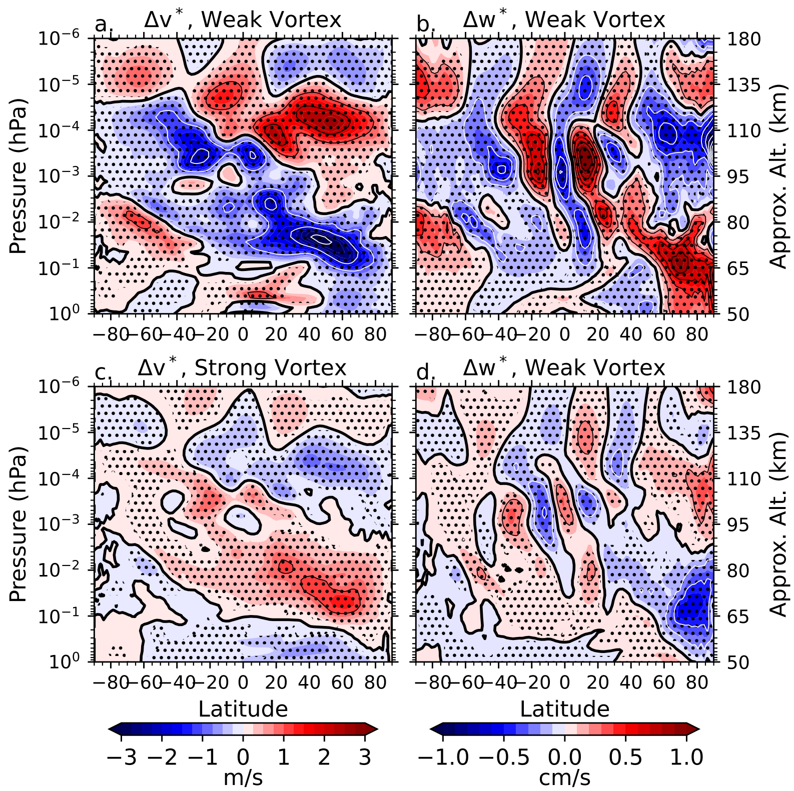

Figure 4. WACCM-X circulation anomalies during weak stratosphere polar vortex events for (a) residual meridional circulation (v^*) and (b) residual vertical circulation (w^*). (c-d) Same as (a-b) except for during strong stratosphere polar vortex events. Stippling denotes areas that are statistically significant at the 95% confidence level. Contour lines are every 1 m/s in v^* and 0.2 cm/s in w^*. The thick black line is the zero contour.

3.2 Ionosphere and Thermosphere

We now turn our attention to understanding how the changes in the MLT tides and circulation influences the ionosphere and thermosphere. Figures 5 and 6 show time series of the SW2 in zonal wind and v^* at 5×10^{-5} hPa, the percentage change in the zonal and diurnal mean height integrated O/N_2, and the SW2 component of TEC for two different Northern Hemisphere winters simulated by WACCM-X. Figure 5 provides an example of a Northern Hemisphere winter with a strong SSW (i.e., weak stratosphere polar vortex) in late January that is preceded by a moderately strong stratosphere polar vortex. There is a notable enhancement in the SW2 at MLT altitudes coincident with the stratosphere polar vortex weakening, which is related to the zonal mean zonal wind and ozone changes that occur during SSWs (Jin et al., 2012; Pedatella et al., 2012; Siddiqui et al., 2019). An enhancement in the SW2 component of the TEC also occurs at the same time, demonstrating the close connection between the SW2 in the MLT winds and in the ionosphere. The enhanced SW2 in the MLT further generates a large change in the residual circulation, with poleward winds evident at middle latitudes in both hemispheres. This is consistent with the residual circulation anomalies during weak stratosphere polar vortex time periods shown in Figures 4a-b. The residual circulation changes in-turn produce a large decrease in the O/N_2 that exceeds 5%, and persists for an extended time period. The results in Figure 5 show that there is also a delay of a few days between the change in the residual circulation and the O/N_2. This delay is consistent with (Pedatella et al., 2016) who also showed a delay between SSW induced circulation anomalies and changes in thermosphere composition.

Figure 6 provides an example of a Northern Hemisphere winter that does not contain a considerably strong or weak stratosphere polar vortex, but is characterized by short term variations in the strength of the stratosphere polar vortex. The relationship between the short-term variability in the stratosphere polar vortex and the SW2 variability is evident in Figure 6a. In general, one can see that times of slightly stronger stratosphere polar vortex are associated with a decreased SW2 amplitude and times with a slightly weaker stratosphere polar vortex are associated with enhanced SW2 amplitudes. However, there are occasions when the relationship between the SW2 amplitude and NAM is not clearly evident. The relationship between the SW2 in the MLT and the ionosphere is again apparent. The circulation anomalies in Figure 6b do not exhibit as clear of a connection with the SW2 in the MLT, though there is a large enhancement in the poleward residual circulation associated with the large SW2 increase around day 50. Likewise, the connection between the short-term variability in the stratosphere polar vortex and the O/N_2 is less evident; however, the general trend of a stronger stratosphere polar vortex generating an increased O/N_2 and a weaker stratosphere polar vortex generating a decreased O/N_2 can be seen in Figure 6c.

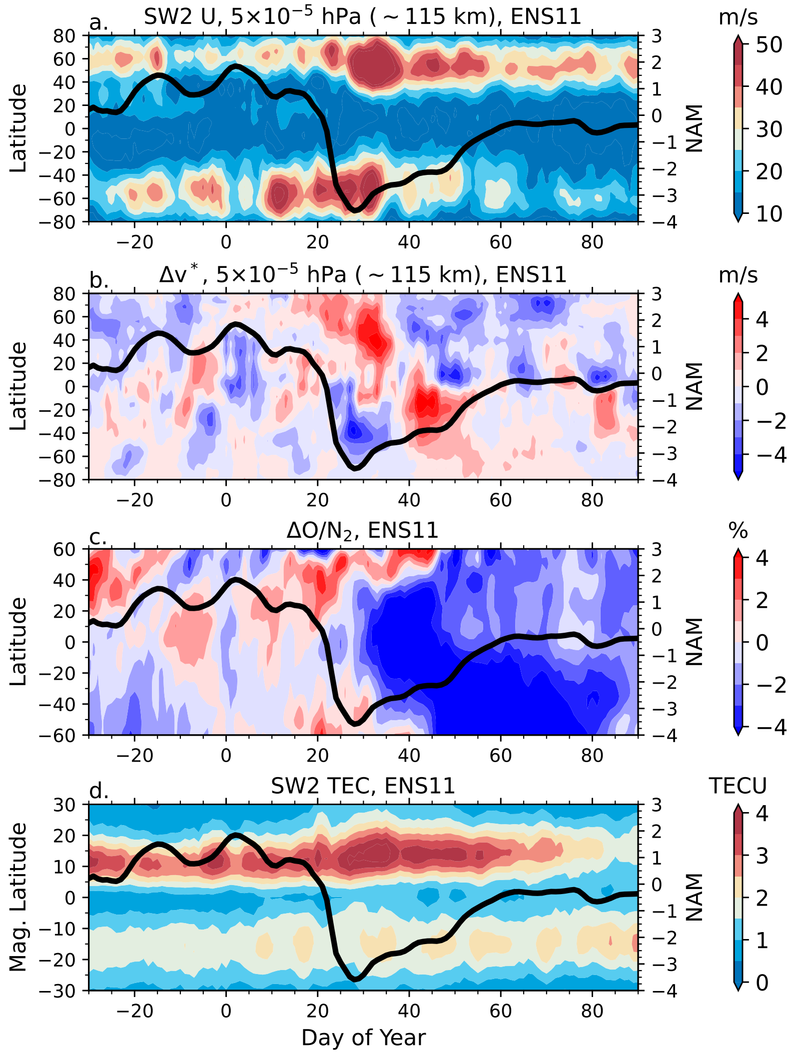

Figure 5. (a) SW2 amplitude in zonal wind at 5×10^{-5} hPa, (b) residual meridional circulation (v^*) at 5×10^{-5} hPa, (c) column integrated O/N_2 anomaly from the seasonal climatology, and (d) SW2 component of TEC. The thick black line is the Northern Annular Mode (NAM) index at 10 hPa. Results are for ensemble member 11.

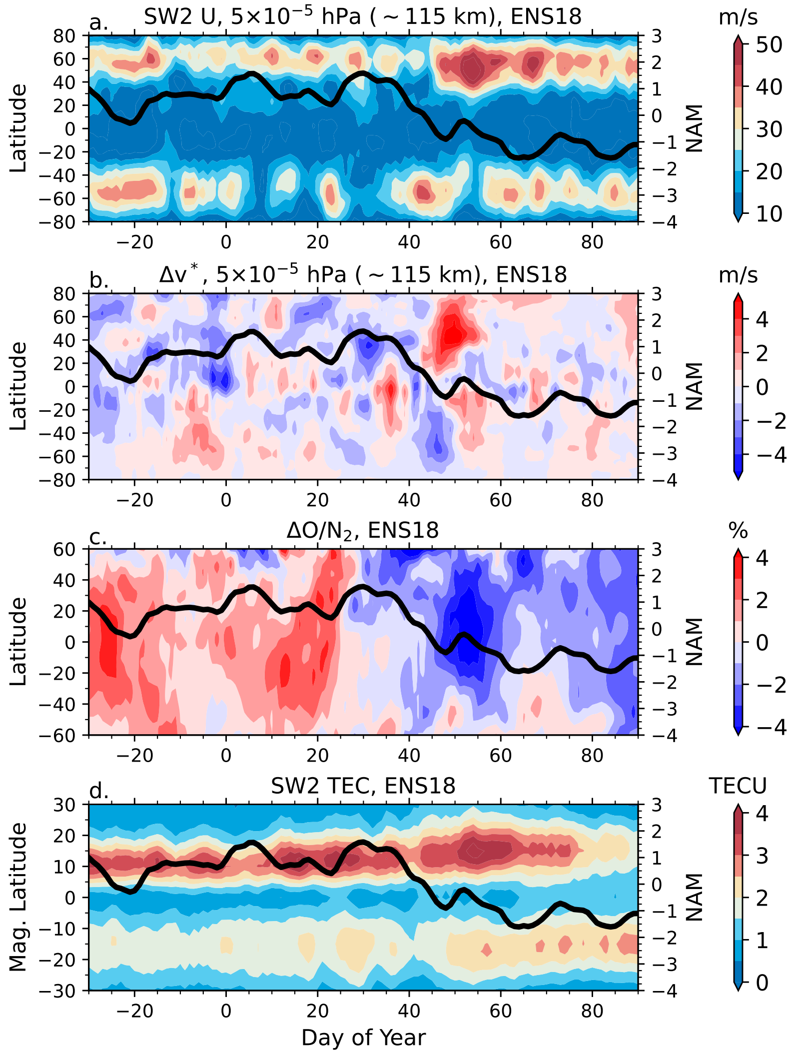

Figure 6. Same as Figure 5 except for the results are shown for ensemble member 18.

Figure 7 shows the average anomalies in O/N_2 and the SW2 component of TEC during weak and strong stratosphere polar vortex time periods. The anomalies are expressed as percentage changes from the climatological background. The results are based on a temporal lag of eight and four days between the NAM and O/N_2 and SW2 component of TEC, respectively. This corresponds to the temporal lag when the correlations maximize. During weak stratosphere polar vortex times, the O/N_2 is, on average, reduced by ∼3-4% at low-latitudes, with smaller decreases at middle latitudes. The O/N_2 response during weak stratosphere polar vortex times in the WACCM-X simulations is slightly smaller than what has been observed during SSWs (Oberheide et al., 2020). This may be due to the fact that the present study includes all stratosphere polar vortex weakenings, and not only large, persistent, SSW events. Alternatively, the model may be underestimating the changes in thermosphere composition, potentially due to known deficiencies in the gravity wave drag parameterization that will influence the MLT circulation (e.g., Stober et al., 2021). An opposite response is seen to occur in the O/N_2 during strong polar vortex time periods, though the magnitude is 1-2%, which is approximately half of the weak stratosphere polar vortex case. If the magnitudes of the response in WACCM-X are equally underestimated compared to observations in both strong and weak stratosphere polar vortex time periods, one may therefore expect up to ∼5% enhancements in equatorial O/N_2 during exceptionally strong stratosphere polar vortex events. Figure 7b shows that the SW2 component of TEC is also notably different during strong and weak stratosphere polar vortex time periods. In particular, the SW2 component of TEC is enhanced by ∼30% in the Northern Hemisphere at low to middle magnetic latitudes, and by 5-15% in the Southern Hemisphere. These enhancements during weak stratosphere polar vortex time periods are generally consistent with the observational results of Oberheide (2022), who showed a stronger response in the Northern Hemisphere and enhancements in the SW2 component of TEC of ∼25-30% during the 2020-2021 SSW. An opposite response is again seen in the SW2 component of TEC during strong stratosphere polar vortex time periods, with decreases of ∼10% occurring at low to middle latitudes. Such a decrease is consistent with the SW2 decrease in the MLT, which can directly influence the SW2 component of TEC through influencing the E-region dynamo.

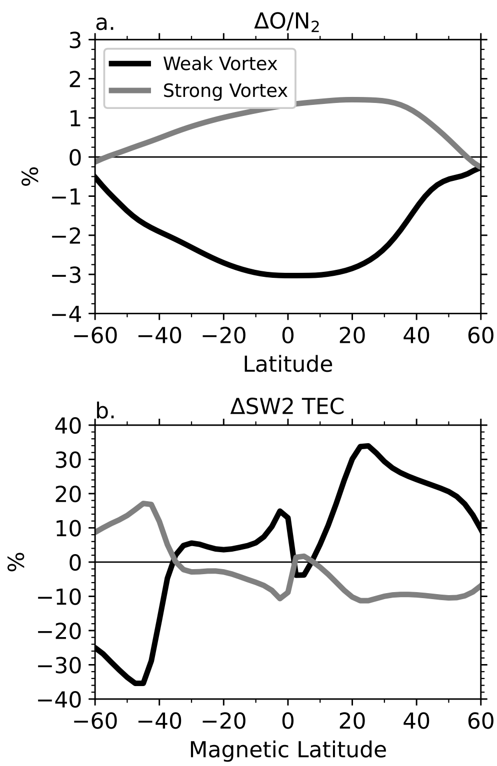

Figure 7. (a) Column integrated O/N_2 anomaly during strong and weak stratosphere polar vortex events. (b) Same as (a) except for the SW2 component of TEC. The results are based on a lag of eight and four days between the NAM at 10 hPa and the O/N_2 and SW2 component of TEC, respectively.

The relationship between the anomalies in column integrated O/N_2 and the SW2 component of TEC and the NAM at 10 hPa is shown in Figure 8. Similar to Figure 7, a lag of eight days is used for O/N_2 and four days for the SW2 component of TEC. The results in Figure 8 are shown based on the O/N_2 anomalies between ±25° geographic latitude and SW2 anomalies between 15-25°N geomagnetic latitude. These regions correspond to where the greatest anomalies occur during the strong and weak stratosphere polar vortex time periods. The results in Figure 8a show a clear relationship between the NAM at 10 hPa and the thermosphere O/N_2, with a positive correlation (i.e., weakening of the stratosphere polar vortex leads to a decrease in O/N_2). The correlation coefficient is 0.54, indicating that the NAM at 10 hPa explains ∼30% of the variability in thermosphere O/N_2 at low latitudes, at least during geomagnetically quiet time periods. An opposite trend is evident in the relationship between the SW2 component of TEC and the NAM at 10 hPa, with a weakening of the stratosphere polar vortex leading to an increase in the SW2 component of TEC. The correlation coefficient between the SW2 component of TEC and the NAM at 10 hPa is -0.42, meaning that ∼18% of the variability in the SW2 component of TEC can be explained by the NAM at 10 hPa. Interestingly, this is similar to the correlation coefficient between the SW2 at middle latitudes in the MLT and the NAM (-0.51 in this study and -0.62 in Pedatella and Harvey (2022)), demonstrating that much of the variability in the SW2 at MLT altitudes is directly transmitted to the low latitude ionosphere.

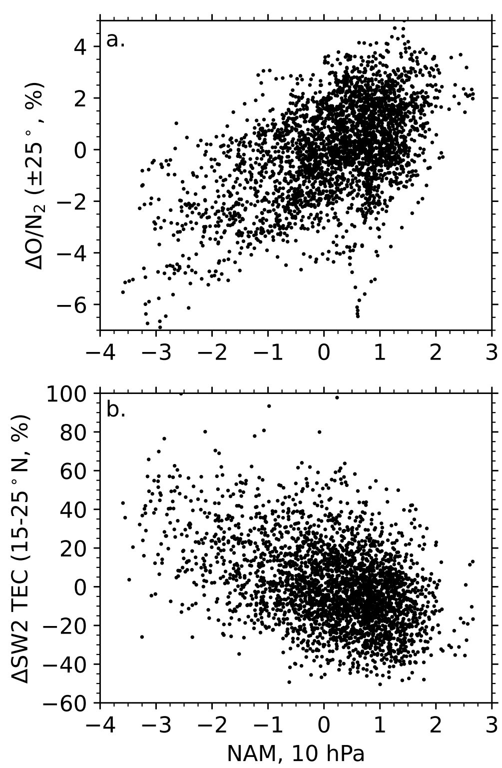

Figure 8. WACCM-X daily column integrated O/N_2 anomaly between ±25° geographic latitude versus the NAM at 10 hPa with a lag of eight days. (b) SW2 amplitude anomaly in TEC between 15-25°N geomagnetic latitude versus the NAM at 10 hPa with a lag of four days. Results are based on the time period December 15 to March 1.

4 Conclusions

The present study demonstrates that variability in the stratosphere polar vortex is connected to changes in the MLT circulation, thermosphere composition, and ionosphere electron densities. While previous studies have shown that SSWs, which are characterized by a weak stratosphere polar vortex, induce changes throughout the middle and upper atmosphere, the present study reveals that the impact of the stratosphere polar vortex variability extends to periods when the stratosphere polar vortex is strong. Based on WACCM-X simulations of 40 Northern Hemisphere winters, we can conclude the following:

1. Weak stratosphere polar vortex periods are characterized by anomalous clockwise and anti-clockwise MLT residual circulations in the Northern Hemisphere and Southern Hemisphere, respectively. The circulation anomalies are reversed during times when the stratosphere polar vortex is strong.

2. The residual circulation anomalies in the MLT generate changes in the diurnal and zonal mean thermosphere column integrated O/N_2. Weak stratosphere polar vortex times are associated with a 3-4% reduction in O/N_2, while strong stratosphere polar vortex time periods are associated with a 1-2% increase in O/N_2.

3. The strength of the stratosphere polar vortex strongly influences the SW2 in the MLT, leading to changes in the SW2 component of TEC at low latitudes. At low latitudes the SW2 amplitude in TEC is increased by ∼20-30% during weak stratosphere polar vortex time periods and decreased by ∼10% during strong stratosphere polar vortex time periods.

4. There is a good correlation between the strength of the stratosphere polar vortex and O/N_2 and the SW2 component of TEC. The NAM at 10 hPa explains ∼30% of the variability in thermosphere O/N_2 and ∼18% of the variability in the SW2 component of TEC during Northern Hemisphere winter and geomagnetically quiet conditions.

The results of the present study during weak stratosphere polar vortex time periods are generally consistent with existing knowledge of variability during SSWs obtained through past modeling and observational studies. It should, however, be noted that the slightly less variable stratosphere polar vortex in the present WACCM-X simulations may lead to underestimating some of the effects. The variability during strong stratosphere polar vortex time periods remains to be observationally confirmed. The changes in SW2 during strong stratosphere polar vortex time periods should be readily detectable by observations given that they can exceed 10%. Limited evidence for the modulation of the SW2 in TEC by the stratosphere polar vortex was presented by Oberheide (2022) for a single winter. The thermosphere O/N_2 changes during strong stratosphere polar vortex time periods may be more difficult to confirm observationally due to their small magnitude, though they may be detectable especially during extremely strong stratosphere polar vortex events, which are underrepresented in the present WACCM-X simulations. More detailed observational studies are therefore required in order to confirm the results of the present study.

Acknowledgments
This material is based upon work supported by the National Center for Atmospheric Research, which is a major facility sponsored by the U.S. National Science Foundation under Cooperative Agreement 1852977. Support from NASA Grant 80NSSC18K1046 and 80NSSC20K1353 are acknowledged.

Open Research

WACCMX is part of the Community Earth System Model (CESM) and the source code is available at https://github.com/ESCOMP/CESM. WACCM-X simulation output used for the present study is available at https://doi.org/10.5281/zenodo.7742051.

References

Baldwin, M. P., Ayarzagüena, B., Birner, T., Butchart, N., Butler, A. H., Charlton-Perez, A. J., … Pedatella, N. M. (2020). Sudden stratospheric warmings. *Reviews of Geophysics*, *n/a*, e2020RG000708. (e2020RG000708 2020RG000708) doi: 10.1029/2020rg000708

Becker, E., Goncharenko, L., Harvey, V. L., & Vadas, S. L. (2022). Multi-step vertical coupling during the january 2017 sudden stratospheric warming. *Journal of Geophysical Research: Space Physics*, *127*, e2022JA030866. (e2022JA030866 2022JA030866) doi: https://doi.org/10.1029/2022JA030866

Chau, J. L., Fejer, B. G., & Goncharenko, L. P. (2009). Quiet variability of equatorial e × b drifts during a sudden stratospheric warming event. *Geophysical Research Letters*, *36*. doi: 10.1029/2008GL036785

Chau, J. L., Goncharenko, L. P., Fejer, B. G., & Liu, H.-L. (2012). Equatorial and low latitude ionospheric effects during sudden stratospheric warming events. *Space Science Reviews*, *168*, 385-417. doi: 10.1007/s11214-011-9797-5

Chau, J. L., Hoffmann, P., Pedatella, N. M., Matthias, V., & Stober, G. (2015). Upper mesospheric lunar tides over middle and high latitudes during sudden stratospheric warming events. *Journal of Geophysical Research: Space Physics*, *120*, 3084-3096. doi: 10.1002/2015JA020998

de la Torre, L., Garcia, R. R., Barriopedro, D., & Chandran, A. (2012). Climatology and characteristics of stratospheric sudden warmings in the whole atmosphere community climate model. *Journal of Geophysical Research: Atmospheres*, *117*. doi: https://doi.org/10.1029/2011JD016840

Fagundes, P. R., Goncharenko, L. P., de Abreu, A. J., Venkatesh, K., Pezzopane, M., de Jesus, R., … Pillat, V. G. (2015). Ionospheric response to the 2009 sudden stratospheric warming over the equatorial, low, and middle latitudes in the south american sector. *Journal of Geophysical Research: Space Physics*, *120*, 7889-7902. doi: 10.1002/2014JA020649

Fang, T.-W., Fuller-Rowell, T., Akmaev, R., Wu, F., Wang, H., & Anderson, D. (2012). Longitudinal variation of ionospheric vertical drifts during the 2009 sudden stratospheric warming. *Journal of Geophysical Research: Space Physics*, *117*. doi: 10.1029/2011JA017348

Fejer, B. G., Olson, M. E., Chau, J. L., Stolle, C., Lühr, H., Goncharenko, L. P., … Nagatsuma, T. (2010). Lunar-dependent equatorial ionospheric electrodynamic effects during sudden stratospheric warmings. *Journal of Geophysical Research: Space Physics*, *115*. doi: 10.1029/2010JA015273

Forbes, J. M. (1982). Atmospheric tide: 2. the solar and lunar semidiurnal components. *Journal of Geophysical Research: Space Physics*, *87*, 5241-5252. doi: https://doi.org/10.1029/JA087iA07p05241

Frissell, N. A., Baker, J. B. H., Ruohoniemi, J. M., Greenwald, R. A., Gerrard, A. J., Miller, E. S., & West, M. L. (2016). Sources and characteristics of medium-scale traveling ionospheric disturbances observed by high-frequency radars in the north american sector. *Journal of Geophysical Research: Space Physics*, *121*, 3722-3739. doi: https://doi.org/10.1002/2015JA022168

Garcia, R. R., Smith, A. K., Kinnison, D. E., Álvaro de la Cámara, & Murphy, D. J. (2017). Modification of the gravity wave parameterization in the whole atmosphere community climate model: Motivation and results. *Journal of the Atmospheric Sciences*, *74*, 275-291. doi: 10.1175/JAS-D-16-0104.1

Gerber, E. P., & Martineau, P. (2018). Quantifying the variability of the annular modes: reanalysis uncertainty vs. sampling uncertainty. *Atmospheric Chemistry and Physics*, *18*, 17099-17117. doi: 10.5194/acp-18-17099-2018

Goncharenko, L. P., Chau, J. L., Liu, H.-L., & Coster, A. J. (2010). Unexpected connections between the stratosphere and ionosphere. *Geophysical Research Letters*, *37*. doi: 10.1029/2010GL043125

Goncharenko, L. P., Harvey, V. L., Liu, H., & Pedatella, N. M. (2021). *Sudden* *stratospheric warming impacts on the ionosphere–thermosphere system.* American Geophysical Union (AGU). doi: https://doi.org/10.1002/9781119815617.ch16

He, M., Chau, J. L., Stober, G., Hall, C. M., Tsutsumi, M., & Hoffmann, P. (2017). Application of manley-rowe relation in analyzing nonlinear interactions between planetary waves and the solar semidiurnal tide during 2009 sudden stratospheric warming event. *Journal of Geophysical Research: Space Physics*, *122*, 10,710-783,795. doi: 10.1002/2017JA024630

Hoffmann, P., Singer, W., Keuer, D., Hocking, W. K., Kunze, M., & Murayama, Y. (2007). Latitudinal and longitudinal variability of mesospheric winds and temperatures during stratospheric warming events. *Journal of Atmospheric and Solar-Terrestrial Physics*, *69*, 2355-2366. (Vertical Coupling in the Atmosphere/Ionosphere System) doi: https://doi.org/10.1016/j.jastp.2007.06.010

Jin, H., Miyoshi, Y., Pancheva, D., Mukhtarov, P., Fujiwara, H., & Shinagawa, H. (2012). Response of migrating tides to the stratospheric sudden warming in 2009 and their effects on the ionosphere studied by a whole atmosphere-ionosphere model gaia with cosmic and timed/saber observations. *Journal of Geophysical Research: Space Physics*, *117*. doi: 10.1029/2012JA017650

Jr., M. J., Forbes, J. M., & Hagan, M. E. (2016). Solar cycle variability in mean thermospheric composition and temperature induced by atmospheric tides. *Journal of Geophysical Research: Space Physics*, *121*, 5837-5855. doi: https://doi.org/10.1002/2016JA022701

Jr., M. J., Siskind, D. E., Drob, D. P., McCormack, J. P., Emmert, J. T., Dhadly, M. S., ... Jacobi, C. (2020). Coupling from the middle atmosphere to the exobase: Dynamical disturbance effects on light chemical species. *Journal of Geophysical Research: Space Physics*, *125*, e2020JA028331. (e2020JA028331 10.1029/2020JA028331) doi: https://doi.org/10.1029/2020JA028331

Körnich, H., & Becker, E. (2010). A simple model for the interhemispheric coupling of the middle atmosphere circulation. *Advances in Space Research*, *45*, 661-668. doi: https://doi.org/10.1016/j.asr.2009.11.001

Limpasuvan, V., Orsolini, Y. J., Chandran, A., Garcia, R. R., & Smith, A. K. (2016). On the composite response of the mlt to major sudden stratospheric warming events with elevated stratopause. *Journal of Geophysical Research: Atmospheres*, *121*, 4518-4537. doi: 10.1002/2015JD024401

Liu, H.-L. (2014). *Waccm-x simulation of tidal and planetary wave variability in the upper atmosphere.* American Geophysical Union (AGU). doi: 10.1002/9781118704417.ch16

Liu, H.-L., Bardeen, C. G., Foster, B. T., Lauritzen, P., Liu, J., Lu, G., ... Wang, W. (2018). Development and validation of the whole atmosphere community climate model with thermosphere and ionosphere extension (waccm-x 2.0). *Journal of Advances in Modeling Earth Systems*, *10*, 381-402. doi: 10.1002/2017MS001232

Liu, H.-L., & Roble, R. G. (2002). A study of a self-generated stratospheric sudden warming and its mesospheric–lower thermospheric impacts using the coupled time-gcm/ccm3. *Journal of Geophysical Research: Atmospheres*, *107*, ACL 15-1-ACL 15-18. doi: 10.1029/2001JD001533

Liu, H.-L., Sassi, F., & Garcia, R. R. (2009). Error growth in a whole atmosphere climate model. *Journal of the Atmospheric Sciences*, *66*, 173-186. doi: 10.1175/2008JAS2825.1

Liu, H.-L., Wang, W., Richmond, A. D., & Roble, R. G. (2010). Ionospheric variability due to planetary waves and tides for solar minimum conditions. *Journal of Geophysical Research: Space Physics*, *115*. doi: https://doi.org/10.1029/2009JA015188

Matsuno, T. (1971). A dynamical model of the stratospheric sudden warming. *Journal of Atmospheric Sciences*, *28*, 1479-1494. doi: 10.1175/

1520-0469(1971)028⟨1479:ADMOTS⟩2.0.CO;2

Maute, A., Hagan, M. E., Richmond, A. D., & Roble, R. G. (2014). Time-gcm study of the ionospheric equatorial vertical drift changes during the 2006 stratospheric sudden warming. *Journal of Geophysical Research: Space Physics*, *119*, 1287-1305. doi: https://doi.org/10.1002/2013JA019490

Miyoshi, Y., Fujiwara, H., Jin, H., & Shinagawa, H. (2015). Impacts of sudden stratospheric warming on general circulation of the thermosphere. *Journal of Geophysical Research: Space Physics*, *120*, 10,810-897,912. doi: https://doi.org/10.1002/2015JA021894

Oberheide, J. (2022). Day-to-day variability of the semidiurnal tide in the f-region ionosphere during the january 2021 ssw from cosmic-2 and icon. *Geophysical Research Letters*, *49*, e2022GL100369. (e2022GL100369 2022GL100369) doi: https://doi.org/10.1029/2022GL100369

Oberheide, J., Pedatella, N. M., Gan, Q., Kumari, K., Burns, A. G., & Eastes, R. W. (2020). Thermospheric composition o/n response to an altered meridional mean circulation during sudden stratospheric warmings observed by gold. *Geophysical Research Letters*, *47*, e2019GL086313. (e2019GL086313 10.1029/2019GL086313) doi: 10.1029/2019GL086313

Orsolini, Y. J., Zhang, J., & Limpasuvan, V. (2022). Abrupt change in the lower thermospheric mean meridional circulation during sudden stratospheric warmings and its impact on trace species. *Journal of Geophysical Research: Atmospheres*, *127*, e2022JD037050. (e2022JD037050 2022JD037050) doi: https://doi.org/10.1029/2022JD037050

Pedatella, N. M., Chau, J. L., Schmidt, H., Goncharenko, L. P., Stolle, C., Hocke, K., ... Siddiqui, T. A. (2018). *How sudden stratospheric warming affects the whole atmosphere.* doi: 10.1029/2018EO092441

Pedatella, N. M., & Harvey, V. L. (2022). Impact of strong and weak stratospheric polar vortices on the mesosphere and lower thermosphere. *Geophysical Research Letters*, *49*, e2022GL098877. (e2022GL098877 2022GL098877) doi: https://doi.org/10.1029/2022GL098877

Pedatella, N. M., & Liu, H. (2013). The influence of atmospheric tide and planetary wave variability during sudden stratosphere warmings on the low latitude ionosphere. *Journal of Geophysical Research: Space Physics*, *118*, 5333-5347. doi: 10.1002/jgra.50492

Pedatella, N. M., & Liu, H.-L. (2018). The influence of internal atmospheric variability on the ionosphere response to a geomagnetic storm. *Geophysical Research Letters*, *45*, 4578-4585. Retrieved from `https://agupubs.onlinelibrary.wiley.com/doi/abs/10.1029/2018GL077867` doi: https://doi.org/10.1029/2018GL077867

Pedatella, N. M., Liu, H.-L., Conte, J. F., Chau, J. L., Hall, C., Jacobi, C., ... Tsutsumi, M. (2021). Migrating semidiurnal tide during the september equinox transition in the northern hemisphere. *Journal of Geophysical Research: Atmospheres*, *126*, e2020JD033822. (e2020JD033822 2020JD033822) doi: https://doi.org/10.1029/2020JD033822

Pedatella, N. M., Liu, H. L., Richmond, A. D., Maute, A., & Fang, T. W. (2012). Simulations of solar and lunar tidal variability in the mesosphere and lower thermosphere during sudden stratosphere warmings and their influence on the low-latitude ionosphere. *Journal of Geophysical Research: Space Physics*, *117*, 1-14. doi: 10.1029/2012JA017858

Pedatella, N. M., & Maute, A. (2015). Impact of the semidiurnal lunar tide on the midlatitude thermospheric wind and ionosphere during sudden stratosphere warmings. *Journal of Geophysical Research: Space Physics*, *120*, 10,710-740,753. doi: 10.1002/2015JA021986

Pedatella, N. M., Richmond, A. D., Maute, A., & Liu, H.-L. (2016). Impact of semidiurnal tidal variability during ssws on the mean state of the ionosphere and thermosphere. *Journal of Geophysical Research: Space Physics*, *121*, 8077-8088. doi: 10.1002/2016JA022910

Siddiqui, T. A., Maute, A., & Pedatella, N. M. (2019). On the importance of interactive ozone chemistry in earth-system models for studying mesophere-lower thermosphere tidal changes during sudden stratospheric warmings. *Journal of Geophysical Research: Space Physics*, *124*, 10690-10707. doi: 10.1029/2019JA027193

Smith, A. K., Pedatella, N. M., & Mullen, Z. K. (2020). Interhemispheric coupling mechanisms in the middle atmosphere of waccm6. *Journal of the Atmospheric Sciences*, *77*, 1101-1118. doi: 10.1175/JAS-D-19-0253.1

Stober, G., Kuchar, A., Pokhotelov, D., Liu, H., Liu, H.-L., Schmidt, H., . . . Mitchell, N. (2021). Interhemispheric differences of mesosphere–lower thermosphere winds and tides investigated from three whole-atmosphere models and meteor radar observations. *Atmospheric Chemistry and Physics*, *21*, 13855-13902. doi: 10.5194/acp-21-13855-2021

Yamazaki, Y., Kosch, M. J., & Emmert, J. T. (2015). Evidence for stratospheric sudden warming effects on the upper thermosphere derived from satellite orbital decay data during 1967–2013. *Geophysical Research Letters*, *42*, 6180-6188. doi: 10.1002/2015GL065395

Yamazaki, Y., & Richmond, A. D. (2013). A theory of ionospheric response to upward-propagating tides: Electrodynamic effects and tidal mixing effects. *Journal of Geophysical Research: Space Physics*, *118*, 5891-5905. doi: 10.1002/jgra.50487

Yiğit, E., Knížová, P. K., Georgieva, K., & Ward, W. (2016). A review of vertical coupling in the atmosphere–ionosphere system: Effects of waves, sudden stratospheric warmings, space weather, and of solar activity. *Journal of Atmospheric and Solar-Terrestrial Physics*, *141*, 1-12. doi: https://doi.org/10.1016/j.jastp.2016.02.011

Zhang, X., & Forbes, J. M. (2014). Lunar tide in the thermosphere and weakening of the northern polar vortex. *Geophysical Research Letters*, *41*, 8201-8207. doi: 10.1002/2014GL062103

Zülicke, C., Becker, E., Matthias, V., Peters, D. H. W., Schmidt, H., Liu, H.-L., . . . Mitchell, D. M. (2018). Coupling of stratospheric warmings with mesospheric coolings in observations and simulations. *Journal of Climate*, *31*, 1107-1133. doi: 10.1175/JCLI-D-17-0047.1

Influence of Stratosphere Polar Vortex Variability on the Mesosphere, Thermosphere, and Ionosphere

N. M. Pedatella[1,2]

[1]High Altitude Observatory, National Center for Atmospheric Research, Boulder, CO, USA.
[2]COSMIC Program Office, University Center for Atmospheric Research, Boulder, CO, USA.

Key Points:

- Investigate the impact of stratosphere polar vortex on the mesosphere and lower thermosphere circulation, ionosphere, and thermosphere.
- Residual circulation in the mesosphere and lower thermosphere is impacted by both strong and weak stratosphere polar vortex events.
- Stratosphere polar vortex explains ∼30% and ∼18% of quiet time variability in thermosphere O/N_2 and ionosphere SW2, respectively.

Corresponding author: Nicholas Pedatella, `nickp@ucar.edu`

Abstract

The Whole Atmosphere Community Climate Model with thermosphere-ionosphere eXtension (WACCM-X) is used to investigate the influence of stratosphere polar vortex variability on the mesosphere, thermosphere, and ionosphere during Northern Hemisphere winter. Based on 40 simulated Northern Hemisphere winters, the mesosphere and lower thermosphere (MLT) residual circulation is found to depend on whether the stratosphere polar vortex is strong or weak. In particular, during weak stratosphere polar vortex time periods, the MLT circulation anomalies are characterized by clockwise and anti-clockwise flow in the Northern and Southern Hemispheres, respectively. Opposite, though weaker, anomalies are found to occur during time periods when the stratosphere polar vortex is strong. The MLT circulation anomalies influence the composition of the lower thermosphere, leading to $\pm 5\%$ changes in the thermosphere column integrated atomic oxygen to molecular nitrogen ratio (O/N_2). Large differences between strong and weak stratosphere polar vortex events are also found to occur in the semidiurnal migrating tide (SW2) in the MLT, which leads to $\pm$15-20% differences in the SW2 component of the ionosphere total electron content (TEC) at low latitudes. The WACCM-X simulation results indicate that variability in the stratosphere polar vortex can explain $\sim$30% and $\sim$18% of the quiet time variability in thermosphere O/N_2 and the SW2 component of TEC during Northern Hemisphere winter, respectively.

1 Introduction

During Northern Hemisphere winter, the stratosphere polar vortex that forms at high-latitudes in the Northern Hemisphere exhibits considerable variability. The stratosphere polar vortex variability is largely due to the presence, or absence, of planetary wave activity. During periods of strong planetary wave activity, the stratosphere polar vortex is weakened, leading to the occurrence of sudden stratosphere warming (SSW) events (Matsuno, 1971). Though identified based on changes in the stratosphere, SSWs have a wide range of impacts throughout the atmosphere (Pedatella et al., 2018; Baldwin et al., 2020).

In the mesosphere and lower thermosphere (MLT), SSW events are associated with changes in the circulation, mean winds, and atmospheric tides. At middle to high latitudes in the Northern Hemisphere, the zonal winds in the MLT reverse direction during SSWs (Liu & Roble, 2002; Hoffmann et al., 2007), which is primarily attributed to changes in gravity wave forcing (Liu & Roble, 2002; Limpasuvan et al., 2016; Zülicke et al., 2018). These zonal wind changes can extend across the equator into the Southern Hemisphere MLT through inter-hemispheric coupling (Körnich & Becker, 2010; Smith et al., 2020). The zonal mean zonal wind changes that occur during SSWs leads to enhancements in the migrating solar (SW2) and lunar (M2) semidiurnal tides (Pedatella et al., 2012; Zhang & Forbes, 2014; Chau et al., 2015). The SW2 is also enhanced due to changes in ozone forcing during SSWs (Siddiqui et al., 2019). Additional tidal variability occurs in non-migrating semidiurnal tides due to the non-linear interactions between the migrating tides and enhanced planetary wave activity (Liu et al., 2010; Pedatella & Liu, 2013; He et al., 2017). The changes in wave forcing during SSWs, including from gravity waves, planetary waves, and tides, alter the mean circulation of the MLT. During SSWs, the MLT circulation is characterized by enhanced clockwise and anti-clockwise circulation patterns in the Northern and Southern Hemispheres, respectively (Miyoshi et al., 2015; Limpasuvan et al., 2016; Orsolini et al., 2022).

The changes that occur in the MLT circulation and tides during SSWs have subsequent effects on the ionosphere and thermosphere. In the equatorial and low latitude ionosphere, there is a pronounced change in the electric fields, vertical plasma drift velocities, and electron densities (Chau et al., 2009; Fejer et al., 2010; Goncharenko et al., 2010). These effects are predominantly driven by changes in the solar and lunar semidiurnal tides and their impact on the E-region dynamo (Fang et al., 2012; Maute et al., 2014). Variations in F-region electron densities also occur at middle latitudes, and are thought to be due to the propagation of enhanced semidiurnal tides into the F-region (Fagundes et al., 2015; Pedatella & Maute, 2015). The magnitude of the ionosphere variations during SSWs can be large, reaching, or even exceeding, 50-100% of climatological values. In contrast, smaller variations (∼5-10%) are observed in the thermosphere neutral composition (atomic Oxygen to molecular Nitrogen ratio, O/N_2) and neutral density (Yamazaki et al., 2015; Oberheide et al., 2020). The thermosphere composition and density changes during SSWs arise due to the aforementioned changes in MLT circulation (Pedatella et al., 2016; Jr. et al., 2020). For a detailed discussion on the effects of SSWs on the middle and upper atmospheres, the reader is referred to the review papers by Chau et al. (2012), Yiğit et al. (2016), and Goncharenko et al. (2021),

The understanding of stratosphere polar vortex variability on the mesosphere, thermosphere, and ionosphere has largely focused on SSW events. However, recent studies have demonstrated that there is a continuum of variability in the middle and upper atmosphere associated with variations in the stratosphere polar vortex. Based on Specified Dynamics Whole Atmosphere Community Climate Model with thermosphere-ionosphere eXtension (SD-WACCM-X) simulations, Pedatella and Harvey (2022) demonstrated that, in addition to weak stratosphere polar vortex events (i.e., SSWs), time periods characterized by a strong stratosphere polar vortex also lead to anomalous zonal mean temperature, winds, and tides in the MLT. Of interest to the present investigation is that Pedatella and Harvey (2022) found the SW2 at middle latitudes in the MLT to be well correlated with the strength of the stratosphere polar vortex across the full range of stratosphere polar vortex variability. This is consistent with Liu (2014), who found a strong correlation between SW2 and zonal mean zonal winds in the high latitude stratosphere. Oberheide (2022) also found a close relationship between the stratosphere polar vortex variability and the SW2 in ionosphere electron density, demonstrating that the influence of the stratosphere polar vortex variability on the SW2 in the MLT subsequently impacts the ionosphere. The strength of the stratosphere polar vortex has also been found to modulate gravity wave activity in the thermosphere and the associated traveling ionosphere disturbances (Frissell et al., 2016; Becker et al., 2022). Specifically, a strong stratosphere polar vortex was found to lead to an enhancement in TIDs while a weak stratosphere polar vortex decreased TID activity.

The present study aims to further investigate how the range of stratosphere polar vortex variability influences the mesosphere, thermosphere, and ionosphere, including both strong and weak stratosphere polar vortex time periods. This is investigated using 40 Northern Hemisphere winters simulated by WACCM-X. The WACCM-X simulations are used to elucidate the influence of strong and weak stratosphere polar vortex time periods on the MLT circulation, thermosphere composition, and ionosphere electron density. The results demonstrate that variability in the stratosphere polar vortex is an important driver of the day-to-day variability in the middle and upper atmosphere during Northern Hemisphere winter, and that these effects are not limited to SSW time periods.

2 WACCM-X Simulations

Analysis of the impact of stratosphere polar vortex variability in the mesosphere, thermosphere, and ionosphere is investigated based on free-running WACCM-X simulations. WACCM-X is a whole atmosphere model that simulates the chemistry, dynamics, electrodynamics, and physics of the Earth's atmosphere from the surface to the upper thermosphere (4.1×10^{-10} hPa). The model horizontal resolution is 1.9° in latitude and 2.5° in longitude. The vertical resolution is ∼1-3 km up to 0.96 hPa, and 0.25 scale heights above this level. A detailed description of WACCM-X can be found in Liu et al. (2018) and is not repeated herein.

The simulations for the present study consist of an ensemble of 40 Northern Hemisphere winters simulated by WACCM-X in its free-running mode. The simulations were initialized from an identical state on October 1. Random perturbations were applied to the model temperature fields at the start of the simulations, which leads to the ensemble members simulating different weather conditions due to chaotic divergence (Liu et al., 2009; Pedatella & Liu, 2018). To eliminate any influence of solar and geomagnetic activity, the simulations were performed with a constant solar flux of 70 solar flux units and a K_p of 0^+. Similar to Pedatella and Harvey (2022), we use the Northern Annular Mode (NAM) at 10 hPa as a measure of the strength of the stratosphere polar vortex. The NAM is calculated based on the polar cap (>65°N) average geopotential height anomalies (Gerber & Martineau, 2018). It is important to note that the NAM in the present study may not be reflective of the true NAM due to the NAM being normalized by the annual mean and the present simulations only covering a portion of the year. As shown in Figure 1, this may lead to a slight difference in the stratosphere (10 hPa) NAM distribution in the WACCM-X ensemble simulations compared to MERRA-2. The different NAM distributions may also be related to differences in the stratosphere zonal mean zonal winds at 10 hPa and 60°N (Figure 1a). In particular, the WACCM-X wind distribution is narrower, which may be related to either fewer mid-winter SSWs simulated in WACCM and/or natural variability (de la Torre et al., 2012; Garcia et al., 2017). This will lead to a narrower NAM distribution as seen in Figure 1b. Given the narrower NAM distribution, the thresholds for strong and weak stratosphere polar vortex events are chosen to be +1.5 and -2.0, respectively. This leads to a roughly similar fraction of strong (13.3%) and weak (4.4%) events as in MERRA-2 when using the thresholds of +2.0 and -3.0 (Pedatella & Harvey, 2022). Similar to Pedatella and Harvey (2022), we present anomalies from the climatology, where the climatology is based on the 40 Northern Hemisphere winter average smoothed with a running 20-day mean. A Student's T-test is used to test the anomalies for statistical significant relative to the anomalies when the stratosphere polar vortex is consider to be neither weak nor strong.

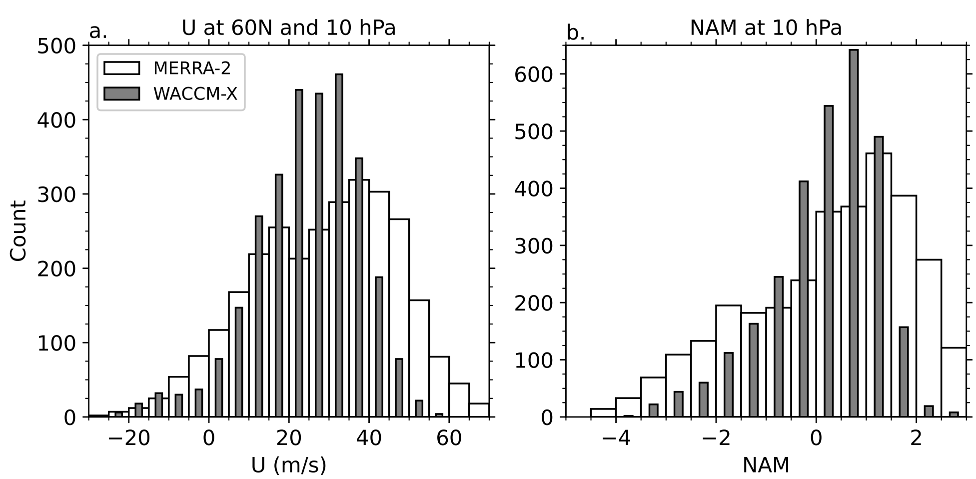

Figure 1. Distribution of (a) zonal mean zonal winds at 60°N and 10 hPa and (b) Northern Annular Mode (NAM) index at 10 hPa during December 15 to March 1 in MERRA-2 (white) and WACCM-X (grey).

3 Results and Discussion

3.1 Mesosphere and Lower Thermosphere

Figure 2 shows the average zonal mean temperature and zonal wind anomalies during strong and weak stratosphere polar vortex time periods. The anomalies are consistent in both magnitude and spatial structure with the results of Pedatella and Harvey (2022). However, the results of Figure 2 are extended into the thermosphere, revealing the temperature and wind anomalies at thermosphere altitudes. They show the expected stratosphere warming, mesosphere cooling, and lower thermosphere warming at high latitudes in the Northern Hemisphere during weak stratosphere polar vortex time periods (e.g., Liu & Roble, 2002), with weaker and opposite signed anomalies during strong stratosphere polar vortex time periods. Extension of the temperature anomalies across the equator into the Southern Hemisphere MLT is also evident. Though there are some minor differences in the equatorial upper stratosphere and lower mesosphere, the zonal mean zonal wind anomalies are also consistent with Pedatella and Harvey (2022). The 40 Northern Hemisphere winters simulated by the free-running WACCM-X thus reproduce the zonal mean anomalies found previously in SD-WACCM-X, which were also shown to be consistent with Aura Microwave Limb Sounder observations. The zonal mean temperature and wind anomalies in Figure 2 reveal anomalies in the middle to upper thermosphere, which were not shown previously in Pedatella and Harvey (2022). During weak stratosphere polar vortex time periods, the thermosphere temperature decreases by $\sim$3-5 K at middle to high latitudes in both hemispheres, and increases by $\sim$2 K at low latitudes. In the thermosphere, the global average temperature decreases by $\sim$2 K, consistent with the observed decrease in satellite drag and neutral mass density (Yamazaki et al., 2015). The decrease is, however, smaller than observed by Yamazaki et al. (2015). A similar temperature pattern, with an increase at low latitudes and decrease at middle to high latitudes, was found to occur due to the influence of atmospheric tides by Jr. et al. (2016). Enhanced semidiurnal tidal amplitudes during weak stratosphere polar vortex time periods may thus explain the temperature structure seen in Figure 2a. In the middle to upper thermosphere, the zonal mean zonal wind anomalies during weak stratosphere polar vortex time periods are westward with maxima of $\sim$10 m/s at middle latitudes near 10^{-5} hPa. This is consistent with previous simulation results (e.g., Pedatella et al., 2016), and is thought to the related to the dissipation of SW2 in the middle thermosphere as will be discussed later. The temperature and zonal wind anomalies in the thermosphere during strong stratosphere polar vortex time periods are small ($<$ 2-3 K or m/s) and generally opposite to those that occur during weak stratosphere polar vortex time periods.

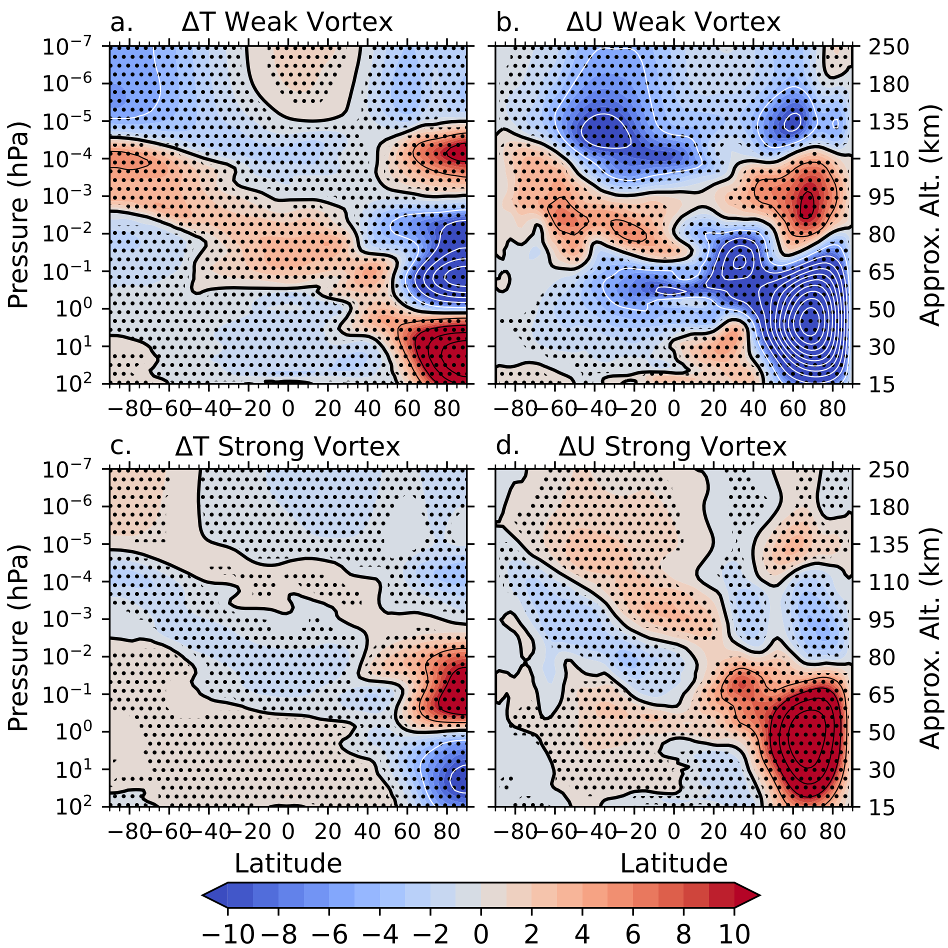

Figure 2. WACCM-X zonal mean anomalies in (a) temperature during weak stratosphere polar vortex times, (b) zonal mean zonal wind during weak stratosphere polar vortex times, (c) temperature during strong stratosphere polar vortex times, and (d) zonal mean zonal wind during strong stratosphere polar vortex times. Stippling denotes areas that are statistically significant at the 95% confidence level. Units are K and m/s for temperature and zonal wind, respectively. Contour lines are every 5 K or m/s, and the thick black line is the zero contour.

Anomalies in the SW2 during strong and weak stratosphere polar vortex time periods are shown in Figure 3. The SW2 anomalies in zonal wind are again largely consistent with Pedatella and Harvey (2022) in the MLT. During weak stratosphere polar vortex time periods, the SW2 in both zonal and meridional wind shows large enhancements in middle latitudes in both hemispheres with maxima between 10^{-4}-10^{-5} hPa (110-130 km). The dissipation of SW2 will tend to drive a westward zonal wind, and the dissipation of the SW2 at these altitudes is thus considered to be a major contributor to the westward zonal mean zonal wind anomalies in Figure 2b. The SW2 enhancements tend to extend into the upper thermosphere. There is, however, a region of decreased SW2 in the Northern Hemisphere middle thermosphere. The decreased SW2 in the middle thermosphere is thought to be due to the impact of the changes in zonal mean zonal winds on the propagation of different Hough modes of SW2 (e.g., Jin et al., 2012). Since the vertical wavelength of the tide impacts its vertical propagation, a change in the dominant modes can change how effectively the SW2 propagates into the middle thermosphere. Changes in the modes of SW2 may also lead to destructive interference, reducing the tidal amplitude (Pedatella et al., 2021). The SW2 anomalies in meridional wind during weak stratosphere polar vortex time periods (Figure 3b) similarity show large enhancements at middle latitudes in the MLT. The additional equatorial enhancement in the SW2 in meridional wind is anticipated due to the latitudinal structure of the SW2 Hough modes being different in zonal and meridional wind (Forbes, 1982). The SW2 meridional wind anomalies exhibit decreased amplitudes at low to middle latitudes ($\sim \pm$10-40°) in the thermosphere, which again may be related to changes in the dominant SW2 Hough modes. The SW2 anomalies during strong stratosphere polar vortex time periods (Figures 3c and 3d) are opposite those of the weak stratosphere polar vortex time periods; however, the magnitudes are smaller. The mechanisms driving the tidal anomalies during weak stratosphere polar vortex time periods are thus acting in the reverse manner during strong stratosphere polar vortex time periods.

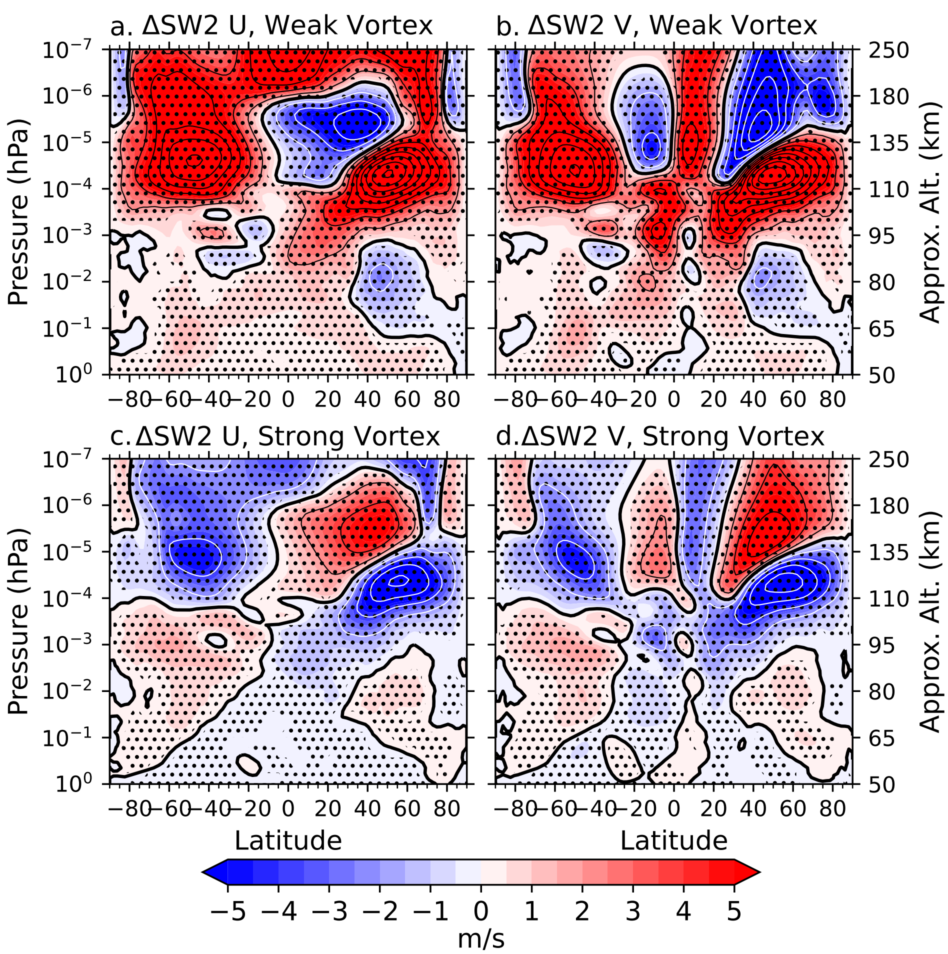

Figure 3. WACCM-X SW2 tidal amplitude anomalies during weak stratosphere polar vortex events for (a) zonal and (b) meridional wind. (c-d) Same as (a-b) except for during strong stratosphere polar vortex events. Stippling denotes areas that are statistically significant at the 95% confidence level. Contour lines are every 2 m/s, and the thick black line is the zero contour.

Changes in the residual meridional (v^*) and vertical ($w*$) circulation during strong and weak stratosphere polar vortex time periods are shown in Figure 4. During weak stratosphere polar vortex time periods, the residual meridional circulation in the Northern Hemisphere has southward anomalies between 10^{-1}-10^{-2} hPa (65-80 km) and northward anomalies at higher altitudes (10^{-3}-10^{-5} hPa, 95-120 km). The spatial structure and the magnitude of the anomalies are consistent with the anomalies that occur during SSWs (Orsolini et al., 2022). The anomalies stretch into the Southern Hemisphere with decreasing amplitude and the boundary between southward and northward anomalies increasing in altitude from the Northern to Southern Hemispheres. This leads to the meridional residual circulation anomalies being oppositely signed in the Northern and Southern Hemispheres at a fixed pressure level (or altitude). Considering also the vertical residual circulation anomalies, one can see that the circulation anomalies during weak stratosphere polar vortex time periods are characterized by a clockwise circulation in the MLT in the Northern Hemisphere, and an anti-clockwise circulation in the Southern Hemisphere MLT. This is again consistent with prior studies (Pedatella et al., 2016). A weak downwelling is also observed in the equatorial region, which is likely due to the dissipation of SW2 (Yamazaki & Richmond, 2013). The residual circulation anomalies during strong stratosphere polar vortex time periods (Figures 4c and 4d) are opposite signed compared to the weak stratosphere polar vortex time periods. The MLT circulation anomalies are thus anti-clockwise in the Northern Hemisphere and clockwise in the Southern Hemisphere during strong stratosphere polar vortex time periods. The reversed circulation anomalies indicates that the impacts of the circulation anomalies on, for example, thermosphere composition and mesosphere chemistry, during strong stratosphere polar vortex time periods will be opposite to those that occur during weak stratosphere polar vortex time periods, though the magnitude of the effects will be smaller.

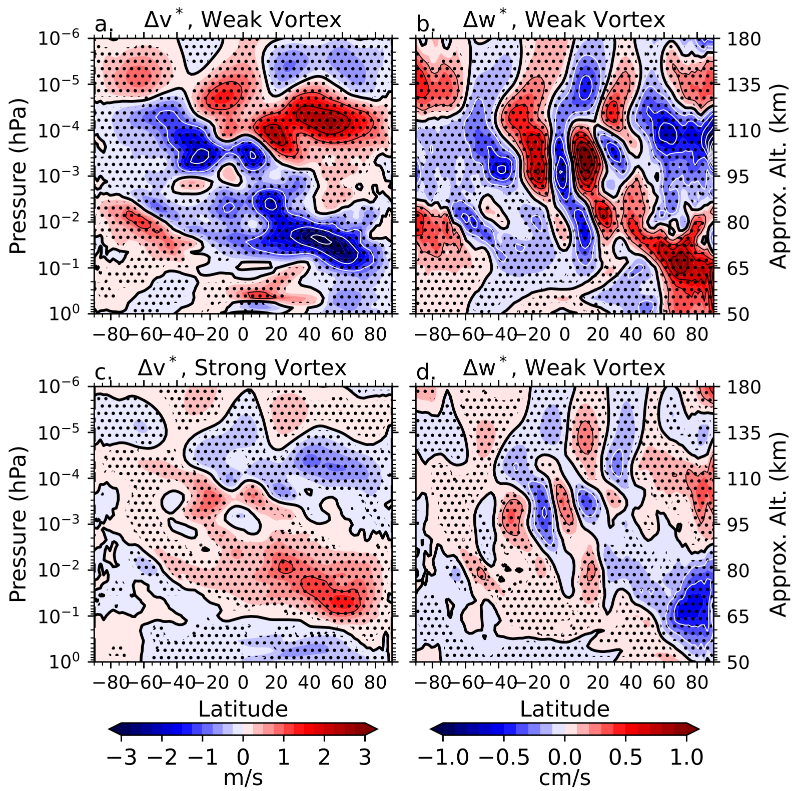

Figure 4. WACCM-X circulation anomalies during weak stratosphere polar vortex events for (a) residual meridional circulation (v^*) and (b) residual vertical circulation (w^*). (c-d) Same as (a-b) except for during strong stratosphere polar vortex events. Stippling denotes areas that are statistically significant at the 95% confidence level. Contour lines are every 1 m/s in v^* and 0.2 cm/s in w^*. The thick black line is the zero contour.

3.2 Ionosphere and Thermosphere

We now turn our attention to understanding how the changes in the MLT tides and circulation influences the ionosphere and thermosphere. Figures 5 and 6 show time series of the SW2 in zonal wind and v^* at 5×10^{-5} hPa, the percentage change in the zonal and diurnal mean height integrated O/N_2, and the SW2 component of TEC for two different Northern Hemisphere winters simulated by WACCM-X. Figure 5 provides an example of a Northern Hemisphere winter with a strong SSW (i.e., weak stratosphere polar vortex) in late January that is preceded by a moderately strong stratosphere polar vortex. There is a notable enhancement in the SW2 at MLT altitudes coincident with the stratosphere polar vortex weakening, which is related to the zonal mean zonal wind and ozone changes that occur during SSWs (Jin et al., 2012; Pedatella et al., 2012; Siddiqui et al., 2019). An enhancement in the SW2 component of the TEC also occurs at the same time, demonstrating the close connection between the SW2 in the MLT winds and in the ionosphere. The enhanced SW2 in the MLT further generates a large change in the residual circulation, with poleward winds evident at middle latitudes in both hemispheres. This is consistent with the residual circulation anomalies during weak stratosphere polar vortex time periods shown in Figures 4a-b. The residual circulation changes in-turn produce a large decrease in the O/N_2 that exceeds 5%, and persists for an extended time period. The results in Figure 5 show that there is also a delay of a few days between the change in the residual circulation and the O/N_2. This delay is consistent with (Pedatella et al., 2016) who also showed a delay between SSW induced circulation anomalies and changes in thermosphere composition.

Figure 6 provides an example of a Northern Hemisphere winter that does not contain a considerably strong or weak stratosphere polar vortex, but is characterized by short term variations in the strength of the stratosphere polar vortex. The relationship between the short-term variability in the stratosphere polar vortex and the SW2 variability is evident in Figure 6a. In general, one can see that times of slightly stronger stratosphere polar vortex are associated with a decreased SW2 amplitude and times with a slightly weaker stratosphere polar vortex are associated with enhanced SW2 amplitudes. However, there are occasions when the relationship between the SW2 amplitude and NAM is not clearly evident. The relationship between the SW2 in the MLT and the ionosphere is again apparent. The circulation anomalies in Figure 6b do not exhibit as clear of a connection with the SW2 in the MLT, though there is a large enhancement in the poleward residual circulation associated with the large SW2 increase around day 50. Likewise, the connection between the short-term variability in the stratosphere polar vortex and the O/N_2 is less evident; however, the general trend of a stronger stratosphere polar vortex generating an increased O/N_2 and a weaker stratosphere polar vortex generating a decreased O/N_2 can be seen in Figure 6c.

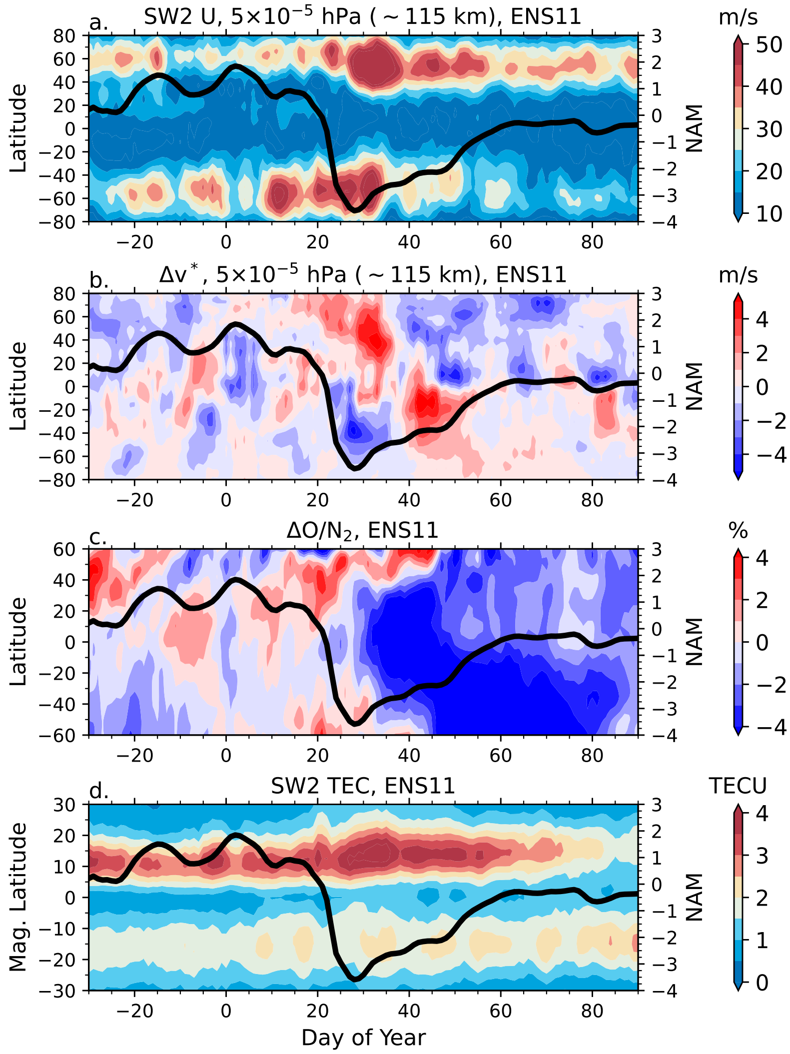

Figure 5. (a) SW2 amplitude in zonal wind at $5{\times}10^{-5}$ hPa, (b) residual meridional circulation (v^*) at $5{\times}10^{-5}$ hPa, (c) column integrated O/N_2 anomaly from the seasonal climatology, and (d) SW2 component of TEC. The thick black line is the Northern Annular Mode (NAM) index at 10 hPa. Results are for ensemble member 11.

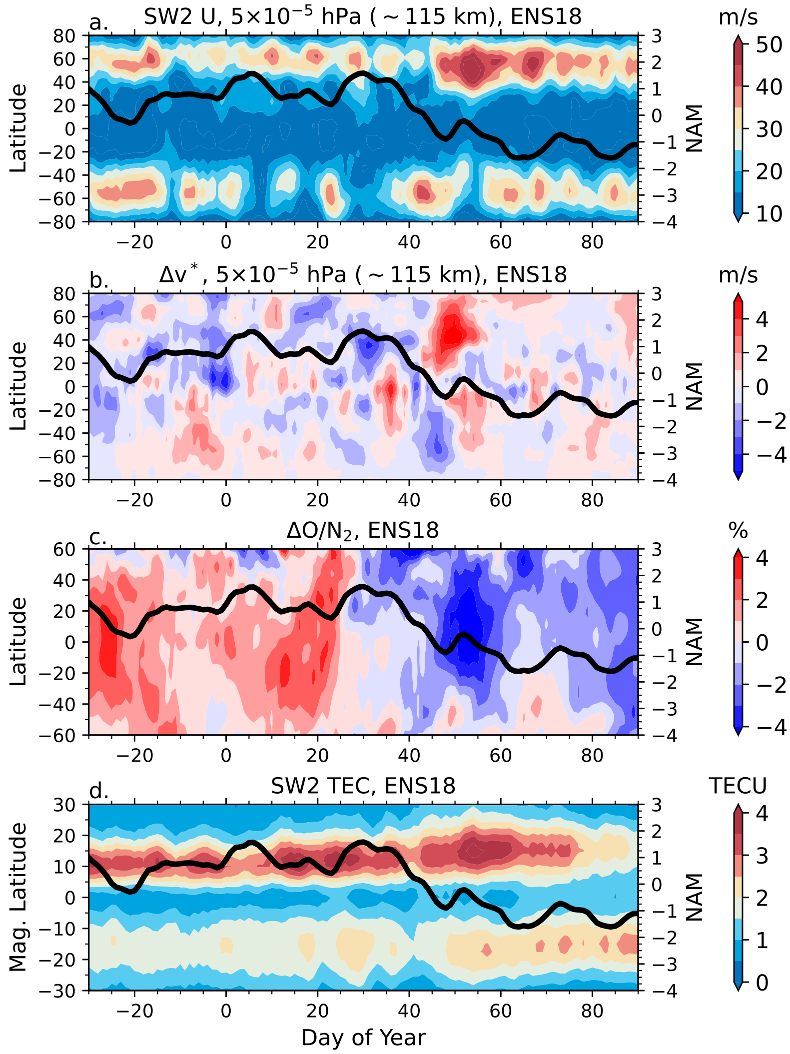

Figure 6. Same as Figure 5 except for the results are shown for ensemble member 18.

Figure 7 shows the average anomalies in O/N_2 and the SW2 component of TEC during weak and strong stratosphere polar vortex time periods. The anomalies are expressed as percentage changes from the climatological background. The results are based on a temporal lag of eight and four days between the NAM and O/N_2 and SW2 component of TEC, respectively. This corresponds to the temporal lag when the correlations maximize. During weak stratosphere polar vortex times, the O/N_2 is, on average, reduced by ∼3-4% at low-latitudes, with smaller decreases at middle latitudes. The O/N_2 response during weak stratosphere polar vortex times in the WACCM-X simulations is slightly smaller than what has been observed during SSWs (Oberheide et al., 2020). This may be due to the fact that the present study includes all stratosphere polar vortex weakenings, and not only large, persistent, SSW events. Alternatively, the model may be underestimating the changes in thermosphere composition, potentially due to known deficiencies in the gravity wave drag parameterization that will influence the MLT circulation (e.g., Stober et al., 2021). An opposite response is seen to occur in the O/N_2 during strong polar vortex time periods, though the magnitude is 1-2%, which is approximately half of the weak stratosphere polar vortex case. If the magnitudes of the response in WACCM-X are equally underestimated compared to observations in both strong and weak stratosphere polar vortex time periods, one may therefore expect up to ∼5% enhancements in equatorial O/N_2 during exceptionally strong stratosphere polar vortex events. Figure 7b shows that the SW2 component of TEC is also notably different during strong and weak stratosphere polar vortex time periods. In particular, the SW2 component of TEC is enhanced by ∼30% in the Northern Hemisphere at low to middle magnetic latitudes, and by 5-15% in the Southern Hemisphere. These enhancements during weak stratosphere polar vortex time periods are generally consistent with the observational results of Oberheide (2022), who showed a stronger response in the Northern Hemisphere and enhancements in the SW2 component of TEC of ∼25-30% during the 2020-2021 SSW. An opposite response is again seen in the SW2 component of TEC during strong stratosphere polar vortex time periods, with decreases of ∼10% occurring at low to middle latitudes. Such a decrease is consistent with the SW2 decrease in the MLT, which can directly influence the SW2 component of TEC through influencing the E-region dynamo.

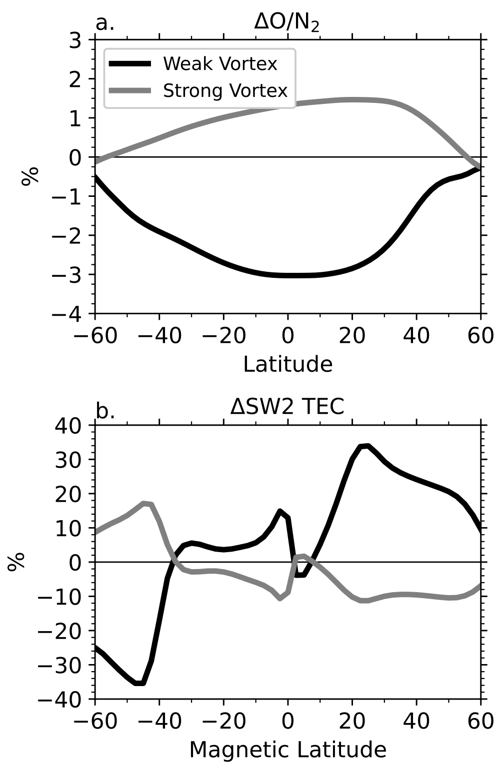

Figure 7. (a) Column integrated O/N_2 anomaly during strong and weak stratosphere polar vortex events. (b) Same as (a) except for the SW2 component of TEC. The results are based on a lag of eight and four days between the NAM at 10 hPa and the O/N_2 and SW2 component of TEC, respectively.

The relationship between the anomalies in column integrated O/N_2 and the SW2 component of TEC and the NAM at 10 hPa is shown in Figure 8. Similar to Figure 7, a lag of eight days is used for O/N_2 and four days for the SW2 component of TEC. The results in Figure 8 are shown based on the O/N_2 anomalies between ±25° geographic latitude and SW2 anomalies between 15-25°N geomagnetic latitude. These regions correspond to where the greatest anomalies occur during the strong and weak stratosphere polar vortex time periods. The results in Figure 8a show a clear relationship between the NAM at 10 hPa and the thermosphere O/N_2, with a positive correlation (i.e., weakening of the stratosphere polar vortex leads to a decrease in O/N_2). The correlation coefficient is 0.54, indicating that the NAM at 10 hPa explains ∼30% of the variability in thermosphere O/N_2 at low latitudes, at least during geomagnetically quiet time periods. An opposite trend is evident in the relationship between the SW2 component of TEC and the NAM at 10 hPa, with a weakening of the stratosphere polar vortex leading to an increase in the SW2 component of TEC. The correlation coefficient between the SW2 component of TEC and the NAM at 10 hPa is -0.42, meaning that ∼18% of the variability in the SW2 component of TEC can be explained by the NAM at 10 hPa. Interestingly, this is similar to the correlation coefficient between the SW2 at middle latitudes in the MLT and the NAM (-0.51 in this study and -0.62 in Pedatella and Harvey (2022)), demonstrating that much of the variability in the SW2 at MLT altitudes is directly transmitted to the low latitude ionosphere.

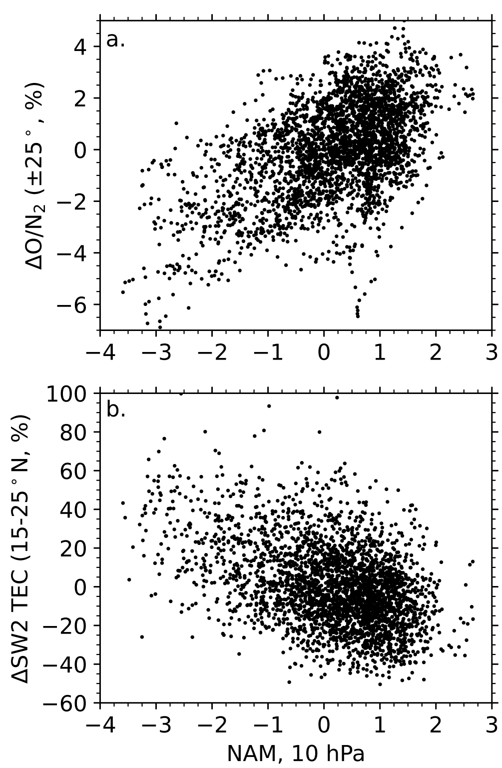

Figure 8. WACCM-X daily column integrated O/N_2 anomaly between ±25° geographic latitude versus the NAM at 10 hPa with a lag of eight days. (b) SW2 amplitude anomaly in TEC between 15-25°N geomagnetic latitude versus the NAM at 10 hPa with a lag of four days. Results are based on the time period December 15 to March 1.

4 Conclusions

The present study demonstrates that variability in the stratosphere polar vortex is connected to changes in the MLT circulation, thermosphere composition, and ionosphere electron densities. While previous studies have shown that SSWs, which are characterized by a weak stratosphere polar vortex, induce changes throughout the middle and upper atmosphere, the present study reveals that the impact of the stratosphere polar vortex variability extends to periods when the stratosphere polar vortex is strong. Based on WACCM-X simulations of 40 Northern Hemisphere winters, we can conclude the following:

1. Weak stratosphere polar vortex periods are characterized by anomalous clockwise and anti-clockwise MLT residual circulations in the Northern Hemisphere and Southern Hemisphere, respectively. The circulation anomalies are reversed during times when the stratosphere polar vortex is strong.

2. The residual circulation anomalies in the MLT generate changes in the diurnal and zonal mean thermosphere column integrated O/N_2. Weak stratosphere polar vortex times are associated with a 3-4% reduction in O/N_2, while strong stratosphere polar vortex time periods are associated with a 1-2% increase in O/N_2.

3. The strength of the stratosphere polar vortex strongly influences the SW2 in the MLT, leading to changes in the SW2 component of TEC at low latitudes. At low latitudes the SW2 amplitude in TEC is increased by ∼20-30% during weak stratosphere polar vortex time periods and decreased by ∼10% during strong stratosphere polar vortex time periods.

4. There is a good correlation between the strength of the stratosphere polar vortex and O/N_2 and the SW2 component of TEC. The NAM at 10 hPa explains ∼30% of the variability in thermosphere O/N_2 and ∼18% of the variability in the SW2 component of TEC during Northern Hemisphere winter and geomagnetically quiet conditions.

The results of the present study during weak stratosphere polar vortex time periods are generally consistent with existing knowledge of variability during SSWs obtained through past modeling and observational studies. It should, however, be noted that the slightly less variable stratosphere polar vortex in the present WACCM-X simulations may lead to underestimating some of the effects. The variability during strong stratosphere polar vortex time periods remains to be observationally confirmed. The changes in SW2 during strong stratosphere polar vortex time periods should be readily detectable by observations given that they can exceed 10%. Limited evidence for the modulation of the SW2 in TEC by the stratosphere polar vortex was presented by Oberheide (2022) for a single winter. The thermosphere O/N_2 changes during strong stratosphere polar vortex time periods may be more difficult to confirm observationally due to their small magnitude, though they may be detectable especially during extremely strong stratosphere polar vortex events, which are underrepresented in the present WACCM-X simulations. More detailed observational studies are therefore required in order to confirm the results of the present study.

Acknowledgments

This material is based upon work supported by the National Center for Atmospheric Research, which is a major facility sponsored by the U.S. National Science Foundation under Cooperative Agreement 1852977. Support from NASA Grant 80NSSC18K1046 and 80NSSC20K1353 are acknowledged.

Open Research

WACCMX is part of the Community Earth System Model (CESM) and the source code is available at https://github.com/ESCOMP/CESM. WACCM-X simulation output used for the present study is available at https://doi.org/10.5281/zenodo.7742051.

References

Baldwin, M. P., Ayarzagüena, B., Birner, T., Butchart, N., Butler, A. H., Charlton-Perez, A. J., ... Pedatella, N. M. (2020). Sudden stratospheric warmings. *Reviews of Geophysics*, *n/a*, e2020RG000708. (e2020RG000708 2020RG000708) doi: 10.1029/2020rg000708

Becker, E., Goncharenko, L., Harvey, V. L., & Vadas, S. L. (2022). Multi-step vertical coupling during the january 2017 sudden stratospheric warming. *Journal of Geophysical Research: Space Physics*, *127*, e2022JA030866. (e2022JA030866 2022JA030866) doi: https://doi.org/10.1029/2022JA030866

Chau, J. L., Fejer, B. G., & Goncharenko, L. P. (2009). Quiet variability of equatorial e × b drifts during a sudden stratospheric warming event. *Geophysical Research Letters*, *36*. doi: 10.1029/2008GL036785

Chau, J. L., Goncharenko, L. P., Fejer, B. G., & Liu, H.-L. (2012). Equatorial and low latitude ionospheric effects during sudden stratospheric warming events. *Space Science Reviews*, *168*, 385-417. doi: 10.1007/s11214-011-9797-5

Chau, J. L., Hoffmann, P., Pedatella, N. M., Matthias, V., & Stober, G. (2015). Upper mesospheric lunar tides over middle and high latitudes during sudden stratospheric warming events. *Journal of Geophysical Research: Space Physics*, *120*, 3084-3096. doi: 10.1002/2015JA020998

de la Torre, L., Garcia, R. R., Barriopedro, D., & Chandran, A. (2012). Climatology and characteristics of stratospheric sudden warmings in the whole atmosphere community climate model. *Journal of Geophysical Research: Atmospheres*, *117*. doi: https://doi.org/10.1029/2011JD016840

Fagundes, P. R., Goncharenko, L. P., de Abreu, A. J., Venkatesh, K., Pezzopane, M., de Jesus, R., ... Pillat, V. G. (2015). Ionospheric response to the 2009 sudden stratospheric warming over the equatorial, low, and middle latitudes in the south american sector. *Journal of Geophysical Research: Space Physics*, *120*, 7889-7902. doi: 10.1002/2014JA020649

Fang, T.-W., Fuller-Rowell, T., Akmaev, R., Wu, F., Wang, H., & Anderson, D. (2012). Longitudinal variation of ionospheric vertical drifts during the 2009 sudden stratospheric warming. *Journal of Geophysical Research: Space Physics*, *117*. doi: 10.1029/2011JA017348

Fejer, B. G., Olson, M. E., Chau, J. L., Stolle, C., Lühr, H., Goncharenko, L. P., ... Nagatsuma, T. (2010). Lunar-dependent equatorial ionospheric electrodynamic effects during sudden stratospheric warmings. *Journal of Geophysical Research: Space Physics*, *115*. doi: 10.1029/2010JA015273

Forbes, J. M. (1982). Atmospheric tide: 2. the solar and lunar semidiurnal components. *Journal of Geophysical Research: Space Physics*, *87*, 5241-5252. doi: https://doi.org/10.1029/JA087iA07p05241

Frissell, N. A., Baker, J. B. H., Ruohoniemi, J. M., Greenwald, R. A., Gerrard, A. J., Miller, E. S., & West, M. L. (2016). Sources and characteristics of medium-scale traveling ionospheric disturbances observed by high-frequency radars in the north american sector. *Journal of Geophysical Research: Space Physics*, *121*, 3722-3739. doi: https://doi.org/10.1002/2015JA022168

Garcia, R. R., Smith, A. K., Kinnison, D. E., Álvaro de la Cámara, & Murphy, D. J. (2017). Modification of the gravity wave parameterization in the whole atmosphere community climate model: Motivation and results. *Journal of the Atmospheric Sciences*, *74*, 275-291. doi: 10.1175/JAS-D-16-0104.1

Gerber, E. P., & Martineau, P. (2018). Quantifying the variability of the annular modes: reanalysis uncertainty vs. sampling uncertainty. *Atmospheric Chemistry and Physics*, *18*, 17099-17117. doi: 10.5194/acp-18-17099-2018

Goncharenko, L. P., Chau, J. L., Liu, H.-L., & Coster, A. J. (2010). Unexpected connections between the stratosphere and ionosphere. *Geophysical Research Letters*, *37*. doi: 10.1029/2010GL043125

Goncharenko, L. P., Harvey, V. L., Liu, H., & Pedatella, N. M. (2021). *Sudden* *stratospheric warming impacts on the ionosphere–thermosphere system.* American Geophysical Union (AGU). doi: https://doi.org/10.1002/9781119815617.ch16

He, M., Chau, J. L., Stober, G., Hall, C. M., Tsutsumi, M., & Hoffmann, P. (2017). Application of manley-rowe relation in analyzing nonlinear interactions between planetary waves and the solar semidiurnal tide during 2009 sudden stratospheric warming event. *Journal of Geophysical Research: Space Physics*, *122*, 10,710-783,795. doi: 10.1002/2017JA024630

Hoffmann, P., Singer, W., Keuer, D., Hocking, W. K., Kunze, M., & Murayama, Y. (2007). Latitudinal and longitudinal variability of mesospheric winds and temperatures during stratospheric warming events. *Journal of Atmospheric and Solar-Terrestrial Physics*, *69*, 2355-2366. (Vertical Coupling in the Atmosphere/Ionosphere System) doi: https://doi.org/10.1016/j.jastp.2007.06.010

Jin, H., Miyoshi, Y., Pancheva, D., Mukhtarov, P., Fujiwara, H., & Shinagawa, H. (2012). Response of migrating tides to the stratospheric sudden warming in 2009 and their effects on the ionosphere studied by a whole atmosphere-ionosphere model gaia with cosmic and timed/saber observations. *Journal of Geophysical Research: Space Physics*, *117*. doi: 10.1029/2012JA017650

Jr., M. J., Forbes, J. M., & Hagan, M. E. (2016). Solar cycle variability in mean thermospheric composition and temperature induced by atmospheric tides. *Journal of Geophysical Research: Space Physics*, *121*, 5837-5855. doi: https://doi.org/10.1002/2016JA022701

Jr., M. J., Siskind, D. E., Drob, D. P., McCormack, J. P., Emmert, J. T., Dhadly, M. S., … Jacobi, C. (2020). Coupling from the middle atmosphere to the exobase: Dynamical disturbance effects on light chemical species. *Journal of Geophysical Research: Space Physics*, *125*, e2020JA028331. (e2020JA028331 10.1029/2020JA028331) doi: https://doi.org/10.1029/2020JA028331

Körnich, H., & Becker, E. (2010). A simple model for the interhemispheric coupling of the middle atmosphere circulation. *Advances in Space Research*, *45*, 661-668. doi: https://doi.org/10.1016/j.asr.2009.11.001

Limpasuvan, V., Orsolini, Y. J., Chandran, A., Garcia, R. R., & Smith, A. K. (2016). On the composite response of the mlt to major sudden stratospheric warming events with elevated stratopause. *Journal of Geophysical Research: Atmospheres*, *121*, 4518-4537. doi: 10.1002/2015JD024401

Liu, H.-L. (2014). *Waccm-x simulation of tidal and planetary wave variability in the upper atmosphere.* American Geophysical Union (AGU). doi: 10.1002/9781118704417.ch16

Liu, H.-L., Bardeen, C. G., Foster, B. T., Lauritzen, P., Liu, J., Lu, G., … Wang, W. (2018). Development and validation of the whole atmosphere community climate model with thermosphere and ionosphere extension (waccm-x 2.0). *Journal of Advances in Modeling Earth Systems*, *10*, 381-402. doi: 10.1002/2017MS001232

Liu, H.-L., & Roble, R. G. (2002). A study of a self-generated stratospheric sudden warming and its mesospheric–lower thermospheric impacts using the coupled time-gcm/ccm3. *Journal of Geophysical Research: Atmospheres*, *107*, ACL 15-1-ACL 15-18. doi: 10.1029/2001JD001533

Liu, H.-L., Sassi, F., & Garcia, R. R. (2009). Error growth in a whole atmosphere climate model. *Journal of the Atmospheric Sciences*, *66*, 173-186. doi: 10.1175/2008JAS2825.1

Liu, H.-L., Wang, W., Richmond, A. D., & Roble, R. G. (2010). Ionospheric variability due to planetary waves and tides for solar minimum conditions. *Journal of Geophysical Research: Space Physics*, *115*. doi: https://doi.org/10.1029/2009JA015188

Matsuno, T. (1971). A dynamical model of the stratospheric sudden warming. *Journal of Atmospheric Sciences*, *28*, 1479-1494. doi: 10.1175/

1520-0469(1971)028⟨1479:ADMOTS⟩2.0.CO;2

Maute, A., Hagan, M. E., Richmond, A. D., & Roble, R. G. (2014). Time-gcm study of the ionospheric equatorial vertical drift changes during the 2006 stratospheric sudden warming. *Journal of Geophysical Research: Space Physics*, *119*, 1287-1305. doi: https://doi.org/10.1002/2013JA019490

Miyoshi, Y., Fujiwara, H., Jin, H., & Shinagawa, H. (2015). Impacts of sudden stratospheric warming on general circulation of the thermosphere. *Journal of Geophysical Research: Space Physics*, *120*, 10,810-897,912. doi: https://doi.org/10.1002/2015JA021894

Oberheide, J. (2022). Day-to-day variability of the semidiurnal tide in the f-region ionosphere during the january 2021 ssw from cosmic-2 and icon. *Geophysical Research Letters*, *49*, e2022GL100369. (e2022GL100369 2022GL100369) doi: https://doi.org/10.1029/2022GL100369

Oberheide, J., Pedatella, N. M., Gan, Q., Kumari, K., Burns, A. G., & Eastes, R. W. (2020). Thermospheric composition o/n response to an altered meridional mean circulation during sudden stratospheric warmings observed by gold. *Geophysical Research Letters*, *47*, e2019GL086313. (e2019GL086313 10.1029/2019GL086313) doi: 10.1029/2019GL086313

Orsolini, Y. J., Zhang, J., & Limpasuvan, V. (2022). Abrupt change in the lower thermospheric mean meridional circulation during sudden stratospheric warmings and its impact on trace species. *Journal of Geophysical Research: Atmospheres*, *127*, e2022JD037050. (e2022JD037050 2022JD037050) doi: https://doi.org/10.1029/2022JD037050

Pedatella, N. M., Chau, J. L., Schmidt, H., Goncharenko, L. P., Stolle, C., Hocke, K., … Siddiqui, T. A. (2018). *How sudden stratospheric warming affects the whole atmosphere.* doi: 10.1029/2018EO092441

Pedatella, N. M., & Harvey, V. L. (2022). Impact of strong and weak stratospheric polar vortices on the mesosphere and lower thermosphere. *Geophysical Research Letters*, *49*, e2022GL098877. (e2022GL098877 2022GL098877) doi: https://doi.org/10.1029/2022GL098877

Pedatella, N. M., & Liu, H. (2013). The influence of atmospheric tide and planetary wave variability during sudden stratosphere warmings on the low latitude ionosphere. *Journal of Geophysical Research: Space Physics*, *118*, 5333-5347. doi: 10.1002/jgra.50492

Pedatella, N. M., & Liu, H.-L. (2018). The influence of internal atmospheric variability on the ionosphere response to a geomagnetic storm. *Geophysical Research Letters*, *45*, 4578-4585. Retrieved from `https://agupubs.onlinelibrary.wiley.com/doi/abs/10.1029/2018GL077867` doi: https://doi.org/10.1029/2018GL077867

Pedatella, N. M., Liu, H.-L., Conte, J. F., Chau, J. L., Hall, C., Jacobi, C., … Tsutsumi, M. (2021). Migrating semidiurnal tide during the september equinox transition in the northern hemisphere. *Journal of Geophysical Research: Atmospheres*, *126*, e2020JD033822. (e2020JD033822 2020JD033822) doi: https://doi.org/10.1029/2020JD033822

Pedatella, N. M., Liu, H. L., Richmond, A. D., Maute, A., & Fang, T. W. (2012). Simulations of solar and lunar tidal variability in the mesosphere and lower thermosphere during sudden stratosphere warmings and their influence on the low-latitude ionosphere. *Journal of Geophysical Research: Space Physics*, *117*, 1-14. doi: 10.1029/2012JA017858

Pedatella, N. M., & Maute, A. (2015). Impact of the semidiurnal lunar tide on the midlatitude thermospheric wind and ionosphere during sudden stratosphere warmings. *Journal of Geophysical Research: Space Physics*, *120*, 10,710-740,753. doi: 10.1002/2015JA021986

Pedatella, N. M., Richmond, A. D., Maute, A., & Liu, H.-L. (2016). Impact of semidiurnal tidal variability during ssws on the mean state of the ionosphere and thermosphere. *Journal of Geophysical Research: Space Physics*, *121*, 8077-8088. doi: 10.1002/2016JA022910

Siddiqui, T. A., Maute, A., & Pedatella, N. M. (2019). On the importance of interactive ozone chemistry in earth-system models for studying mesophere-lower thermosphere tidal changes during sudden stratospheric warmings. *Journal of Geophysical Research: Space Physics*, *124*, 10690-10707. doi: 10.1029/2019JA027193

Smith, A. K., Pedatella, N. M., & Mullen, Z. K. (2020). Interhemispheric coupling mechanisms in the middle atmosphere of waccm6. *Journal of the Atmospheric Sciences*, *77*, 1101-1118. doi: 10.1175/JAS-D-19-0253.1

Stober, G., Kuchar, A., Pokhotelov, D., Liu, H., Liu, H.-L., Schmidt, H., ... Mitchell, N. (2021). Interhemispheric differences of mesosphere–lower thermosphere winds and tides investigated from three whole-atmosphere models and meteor radar observations. *Atmospheric Chemistry and Physics*, *21*, 13855-13902. doi: 10.5194/acp-21-13855-2021

Yamazaki, Y., Kosch, M. J., & Emmert, J. T. (2015). Evidence for stratospheric sudden warming effects on the upper thermosphere derived from satellite orbital decay data during 1967–2013. *Geophysical Research Letters*, *42*, 6180-6188. doi: 10.1002/2015GL065395

Yamazaki, Y., & Richmond, A. D. (2013). A theory of ionospheric response to upward-propagating tides: Electrodynamic effects and tidal mixing effects. *Journal of Geophysical Research: Space Physics*, *118*, 5891-5905. doi: 10.1002/jgra.50487

Yiğit, E., Knížová, P. K., Georgieva, K., & Ward, W. (2016). A review of vertical coupling in the atmosphere–ionosphere system: Effects of waves, sudden stratospheric warmings, space weather, and of solar activity. *Journal of Atmospheric and Solar-Terrestrial Physics*, *141*, 1-12. doi: https://doi.org/10.1016/j.jastp.2016.02.011

Zhang, X., & Forbes, J. M. (2014). Lunar tide in the thermosphere and weakening of the northern polar vortex. *Geophysical Research Letters*, *41*, 8201-8207. doi: 10.1002/2014GL062103

Zülicke, C., Becker, E., Matthias, V., Peters, D. H. W., Schmidt, H., Liu, H.-L., ... Mitchell, D. M. (2018). Coupling of stratospheric warmings with mesospheric coolings in observations and simulations. *Journal of Climate*, *31*, 1107-1133. doi: 10.1175/JCLI-D-17-0047.1